Kos'yan, R.; Kunz, Hans; Pykhov, N.; Kuznetsov, Ivan; Podymov, I.; Vorobyev, P.

Konzentration und Transport suspendierter Sedimente bei unregelmäßigem Seegang

Die Küste

Zur Verfügung gestellt in Kooperation mit/Provided in Cooperation with:
Kuratorium für Forschung im Küsteningenieurwesen (KFKI)

Verfügbar unter/Available at: https://hdl.handle.net/20.500.11970/101457

Vorgeschlagene Zitierweise/Suggested citation:
Kos'yan, R.; Kunz, Hans; Pykhov, N.; Kuznetsov, Ivan; Podymov, I.; Vorobyev, P. (2001): Konzentration und Transport suspendierter Sedimente bei unregelmäßigem Seegang. In: Die Küste 64. Heide, Holstein: Boyens. S. 161-200.

Die Küste, 64 (2001), 161-200

Physical regularities for the suspension and transport of sand under irregular waves

Kos'yan, R.[2], Kunz, H.[1], Pykhov, N.[3], Kuznetsov, S.[3], Podymov, I.[2] u. P. Vorobyev[3]

Zusammenfassung

Konzentration und Transport suspendierter Sedimente bei unregelmäßigem Seegang

Durch den Energieeintrag von Wellen wird Sand an der Sohle bewegt und in Suspension gebracht. Diese Prozesse wurden für Flachwasserseegang durch Naturmessungen in der Brecherzone von Küsten des Schwarzen Meeres (Novomichailovka'93), der Nordsee (Norderney'94) und des Mittelmeeres (EbroDelta'96) aufgezeichnet. Die Naturmessungen auf Norderney waren in das vom BMBF geförderte KFKI-Verbund-Forschungsvorhaben „Vorstrand- und Strandauffüllungen im Bereich von Buhnen-Deckwerk-Systemen" eingebunden.

Die Messdaten beschreiben, wie sich die Konzentrationen suspendierter Stoffe und des im sohlnahen Bereich mobilisierten Sandes unter dem Einfluss von unregelmäßigem Seegang verändern. Die jeweils im vertikalen Messprofil erfassten zeitlichen Veränderungen der Konzentrationsverteilung der Sedimente wurden in Beziehung gestellt zu den längs und quer zur Uferlinie gerichteten Strömungsgeschwindigkeiten. Betrachtet wurden unterschiedliche Energiezustände des Seegangs, und es erfolgte eine Einteilung in Frequenzbereiche bezogen auf eine ermittelte „Grenzfrequenz". Auf dieser Grundlage wurden Zusammenhänge untersucht, über die auf physikalische Prozesse der Suspensionsverteilung und des Sedimenttransportes rückgeschlossen werden konnte. Erkenntnisse zu diesen Prozessen sind unverzichtbar, um numerische Modelle zur Simulation der Sandbewegung fortzuentwickeln und dabei besonders auch Transportmodelle, die man in der Praxis für eine Optimierung von Strand- und Vorstrandauffüllungen verwenden kann.

Die Messungen erfolgten in mehreren Vertikalprofilen, die sich auf einer Senkrechten zur Uferlinie verteilen. Es wurden zeitlich hochauflösende optische und elektromagnetische Sensoren eingesetzt, mit denen die Stoff-Konzentration (Sand im sohlnahen Bereich und in Suspension), die Strömungsgeschwindigkeit (Vektor) und der Wasserstand (Seegang) im Vertikalprofil in unterschiedlichen Tiefen aufgezeichnet wurden. Zur messtechnischen Erfassung der Suspensionskonzentration konnte während der Kampagne „Norderney'94" erstmals ein neu entwickeltes Gerät („Turbidimeter") unter Tidebedingungen betrieben werden. Durch die Zusammenführung der Daten aus Messkampagnen in den drei unterschiedlichen Untersuchungsgebieten gelang es, die komplexen physikalischen Prozesse des Transportes und der Suspension unter unregelmäßigen Wellen in der Vorstrand- und Strandzone (Brecher- oder Brandungszone) zu beschreiben und besser zu verstehen.

Die Untersuchungen erstreckten sich sowohl auf die Vorgänge des Sandtransportes unter Wellen, die in flaches Wasser einlaufen und dabei durch den physikalischen Vorgang des „shoaling" verformt werden, als auch auf Wellen, die brechen (Schwall- und Sturzbrecher). Von besonderem Interesse sind Messzeiten, zu denen der Vorgang des Brechens im Bereich eines Messprofils (Brechpunkt) erfolgt. Hierzu werden Beispiele dargestellt und Untersuchungsergebnisse erläutert. Die verschieden großen Energieeinträge durch Wellen und die dadurch verursachte sohlnahe Strömungsgeschwindigkeit kann unterschiedlichen Sohlformen zugeordnet werden.

[1] Coastal Research Station, Lower Saxony State Agency for Ecology. An der Muehle 5, D-26548 Norderney, Germany.

[2] The Southern Branch of the P.P. Shirshov Institute of Oceanology, Russian Academy of Sciences. 353470 Gelendzhik – 7, Russia.

[3] P. P. Shirshov Institute of Oceanology, Russian Academy of Sciences. Nakhimovskiy prospectus 36, 117859 Moscow, Russia.

Die Küste, 64 (2001), 161-200

Die Sohlform wiederum beeinflusst den sohlnahen Prozess der Sedimentaufwirbelung und die Verteilung der Suspensionskonzentration in der messtechnisch erfassten Wassersäule. Die Charakterisierung der unterschiedenen Zustände (Typen) erfolgte daher durch die kombinierte Ausweisung von Wellenenergie (Turbulenzintensität, Wirbelstruktur) als „klein" (Low Energetic Conditions) und „groß" (High Energetic Conditions) sowie der Sohlform (glatt, 2D-Riffel, 3D-Riffel).

Für die typisierten Zustände sind beispielhaft der zeitliche Verlauf von Geschwindigkeiten und Suspensionskonzentrationen sowie Spektrum, Phasenverschiebung und Zusammenhang (Korrelation) dargestellt. Die gewählte unterschiedliche zeitliche Auflösung für die Untersuchungen ergibt für die hier vorgestellten Zeitfenster eine Dauer von zwei bis zu sechshundert Sekunden. Die vergleichende Auswertung der Größen erbringt Erkenntnisse für die Beantwortung der Frage, wie straff die Zusammenhänge zwischen Einflussgrößen (insbesondere Strömungsgeschwindigkeit) und Suspensionskonzentration sind. So wurde festgestellt, dass nur ein schwacher Zusammenhang zwischen der Sedimentkonzentration und der Strömungsgeschwindigkeit senkrecht zum Strand (Querströmung) besteht. Als Konsequenz ergibt sich somit für die aktive Zone des Strandes und Vorstrandes (surf zone), dass es zweifelhaft ist, ob man für Berechnungen der Suspensions-Transportrate die sogenannte „Bezugskonzentration an der Sohle" verwenden kann, wie dies in bestehenden Modellen geschieht. Für die energieschwächere „Shoaling-Zone" hingegen konnte bestätigt werden, dass es eine recht gute Korrelation zwischen Suspensions-Konzentration und Querströmung gibt, so dass hier die Zweifel nicht begründet sind. Die mit den Naturmessdaten ermittelten Suspensionsfrachten senkrecht zur Strandlinie sind beispielhaft dargestellt und ursächlich erklärt. Diesen sind Ergebnisse gegenübergestellt, die mit einem Ansatz berechnet wurden, der eine „Bezugskonzentration an der Sohle" verwendet (Bailard Model). Eine vergleichende Auswertung quantifiziert das zuvor allgemein vorgestellte Ergebnis.

Abstract

The processes which control the temporal variability of the suspended sand concentration and the sand flux near the bottom have been investigated by using field data. The information on the suspended sediment concentration and components of the fluid velocity were recorded synchronously by optical and electromagnetic sensors with a high frequency response. The data have been collected during the field experiments "Novomichailovka '93" (Black Sea), "Norderney'94" (North Sea) and "Ebrodelta'96" (Mediterranean Sea).

Concerning the bottom, two bed conditions have been distinguished: the rippled bed and the flat bottom. For the rippled bed condition, the lee vortex ejection is a mechanism which forces sand into suspension. High correlation has been observed between the time-varying sediment concentration of the suspension and the cross-shore velocity at the frequency of the spectral peak. A comparable coherence has been confirmed for the envelope of the cross shore velocities and for the peak of the wave group spectrum. The sediment concentration fluctuation at the frequency of the wave spectral peak lags on phase compared with the peak of the cross-shore velocity with the time of $-\pi/2$ for 2D ripples and of $-\pi/3$ for 3D ripples.

For the flat bed condition with high nearbottom velocities, the vortex ejection due to shear instability of the bottom boundary layer is the most probable mechanism which leads to the suspension of sand. The recorded time series for the sediment concentration correlate well with the cross-shore velocities and lag on phase by $-\pi/4$ with respect to the frequency of the peak of the wave spectrum.

The recorded field data show how the physical process of sand suspension in the surf zone under the condition of breaking waves is caused by the generated macroturbulent vortices which penetrate from the water surface to the bottom. The analysed records demonstrate and explain that the concentration fluctuation of the suspended sediment correlates well with the turbulent kinetic energy and correlates very little with the cross shore directed velocity or its envelope. For the special case of plunging breakers, the records describe how the vertical sediment flux is created by the wave induced vertical velocity component.

The field experiments provide sound data, which describe and explain the complex physical processes of sand suspension and transport under irregular waves. The results will be used to improve existing formulae which can be applied to coastal engineering problems.

Die Küste, 64 (2001), 161-200

Inhalt

1. Introduction

The enormous amount of energy stored in waves is predominantly transformed by breaking processes, both in the shallow nearshore zone and on the shore itself. The dissipation of wave energy in this zone generates water motions of various scales, such as small-scale turbulence, large-scale vortices, long-period waves, cross and longshore currents. These scales affect the intensity and direction of the sediment transport. The complex pattern of water motion and the related sand transport determines the morphological development of the nearshore zone and the shoreline.

During storm, the main part of the sand transport occurs in a suspended state. This transport of sandy and silty sediment has a strong impact on beaches, sea channels, ports, pipelines etc. and it affects the coastal environment. Consequently, the quantitative prediction of the concentration and the transport rate of suspended sand under irregular waves is one of the fundamental problems of coastal zone dynamics. Hence, it has attracted specific attention of numerous scientists.

A time averaged approach for the prediction of the suspended sand concentration and the suspended sand transport rate has been adopted by many researchers (KOS'YAN and PYKHOV, 1991). During the last 30 years a good number of formulae have been published which assess or estimate the value of suspended sediment concentrations and rates. The fact is, that no universal dependencies can be recognized from the recorded data. This is due to the lack of clear physical notions about the mechanisms of sand stirred and transported under irregular waves above plane and rippled beds (KOS'YAN, KUZNETSOV and PYKHOV, 1994).

It is now widely accepted that satisfactory results cannot be obtained only on the basis of mean values. From the physical point of view, such an approach is inaccurate because it does not take into account the real mechanisms of sand suspension and the contribution for the wave induced velocities to the net flux of the suspended sediment. The phase relationship between the fluctuations of suspended sediment concentration and the velocity has a significant influence on the magnitude and the direction of an oscillatory suspended sediment flux and its contribution to the net flux.

Different approaches are used for the prediction of the time-space variations of the suspended sand concentration during a wave cycle: mixing length approach (BAKKER, 1974; RIBBERINK and EL-SALEM, 1995); eddy viscosity approach (FREDSOE et al., 1985; DEIGAARD et al., 1986); turbulent k and k–e closure schemes (HAGATUN and EIDSVIK, 1988; DAVIES, 1992; DAVIES and LI, 1997); vortex type models (HANSEN et al., 1994). In these approaches the tem-

Die Küste, 64 (2001), 161-200

poral-spatial variations of the suspended sand concentration are determined by the turbulent diffusion and by introducing a time varying reference concentration. The reference concentration is drawn from the bed shear stress, which is calculated by applying currently used formulae.

Most of the models based on the addressed approaches are satisfactorily valid only for high energetic flows with the restriction that the bed has to remain flat and that a sheet flow layer exists at the water-sediment interface. Those conditions exist under highly deformed unbroken waves. In such a case the turbulent diffusion should provide an appropriate base to model the structure of the boundary layer and the associated distribution of the suspended sand concentration in the sheet flow layer. However, a more or less extended suspension layer exists above the thin sheet flow layer and interacts with it. The temporal variations of the suspended sand concentration in this layer are determined by convective suspension events during the time of flow deceleration and during the reversals of the velocity (MURRAY et al., 1991; RIBBERINK and EL-SALEM, 1995). These processes are not predicted by the existing models. Up to now, none of the models provides a sufficiently detailed description on how the concentration of suspended sand changes in time just above the sheet flow layer.

To estimate the rates of sediment transport, a quasi-steady energetic approach (BAILARD, 1981) is widely used. In this approach, the sediment transport rate is proportional to the 3^{rd}–5^{th} moment of the near bottom water velocity. It is useful for practical applications, due to its simplicity, although it does not represent the physical processes correctly. Such models ignore a time varying description of the velocity and the concentration fields and they cannot provide a detailed description of suspension events, such as phase shifts between velocity and concentration fluctuations and vertical structures of the net suspended sediment flux under real wave conditions. Measured data often significantly differ from the calculated ones (SOULSBY, 1995; KUZNETSOV and PYKHOV, 1998). In the surf zone, the dependency of the sand concentration on the energy dissipation due to wave breaking has to be considered in addition to the energy dissipation caused by bottom friction. Probably, it will be possible to improve the existing models by taking into account the corresponding phase lag between the sediment concentration and the velocity for each of the sand suspending mechanisms.

Generally, the temporal variability of the sand concentration in a measurement point is determined by the coherence of locally induced sand suspension from the bottom, the diffusion of suspended sediments and the advection by water vortices which transport suspended material.

From the physical point of view, it is a necessary assumption, that the particles are forced into suspension: an instantaneous water flow must be present with a vertical velocity component directed upward from the bottom which is larger than the settling velocity of the sand particle. Three basic mechanisms of suspension of sand can be distinguished from the results of laboratory investigations with monochromatic waves:

The first mechanism is the suspension of sand by vortices, which are formed behind the ripple crests. For the case of 2-D vortex ripples at the bottom, the lee vortices eject sand from the bottom twice per wave period at the moment of flow reversal. In this case, the suspended sand concentration has a phase lag of approximately $-\pi/2$ in relation to the maximum of the cross-shore velocity (NIELSEN, 1991; SLEATH, 1984). At the present time, there are no measurements available for the case of 3-D vortex ripples, which describe the temporal variations of the suspended sand concentration in the unsteady wave induced flow. Observations for the case of the steady flow have shown, that in this case the suspension of sand is determined by 3-D horse-shoe vortices, which are formed behind the ripple crest, and which quasi-periodically eject particles into the water column (SYUNSUKE and ASAEDA, 1983).

The second mechanism is the suspension of sand by vortices which are formed due to an instability of the sheet flow boundary layer over a nearly plane bottom during the flow deceleration. Laboratory studies of the turbulence in an oscillatory bottom boundary layer above a slightly rough bottom (HINO et al., 1983) have shown a sharp increase of the turbulence intensity during the flow deceleration and at the time of the flow reversals. Visual observations have shown the presence of horse-shoe vortices and the associated ejection of sediment during the flow deceleration phase (HINO et al., 1983). According to the experimental data of HINO et al. (1983) and CONLEY and INMAN (1992), the time lag of the burst of turbulence relatively to the extremum of the velocity is about 1/8 of the flow oscillation period.

The third mechanism is the suspension of sand by large-scale vortices with a horizontally or vertically inclined axis which are formed under plunging and spilling breakers (NADAOKA and KONDOH, 1989; ZHANG et al., 1994; PYKHOV et al., 1995). Plunging breakers are characterized by a jet impinging on the oncoming trough and the subsequent violent transition from the irrotational to the rotational motions (vortices) with horizontal axis. Spilling breakers occur as broken water spilling from the front face of the wave and differ fundamentally from the plunging breakers. Spilling breakers predominantly produce vortices with a vertically inclined axis. Such vortices expand to the bottom and catch the sand from the bottom like a tornado (KOS'YAN, 1988; ZHANG et al., 1994). Investigations of the temporal variability of the turbulence in breakers show, that the turbulence dies out between bores in case of the plunging breaker and that the turbulence decay time is large in comparison to the wave period-time of spilling breakers (TING and KIRBY, 1994; 1995; 1996).

In order to model the rate and the direction of a sediment transport, it is very important to understand the time scales of the turbulent kinetic energy (TKE) fluctuation and the variations of the suspended sediment concentration. The same accounts for the phase relationship between these parameters and the near-bottom water velocity. The majority of investigators share the hypothesis about sediment suspension by vortices, but the confirmation of this fact by direct field measurements is poor up to now. The mechanism of suspension of sediment by the turbulence of vortices has been verified by some measurements of the macro turbulence under irregular waves in the surf zone (GEORGE et al., 1994; RODRIGUEZ et al., 1995). The results of this research gave a possibility to assess a time averaged value of the turbulent kinetic energy of the integral length scale and of the turbulent viscosity. But they did not allow to trace the temporal variability of these parameters, which are necessary for the analysis of temporal fluctuations of the suspended sediment concentrations and the transport rates.

Under field conditions the production of turbulent vortices is affected by the group structure of gravity waves, by infragravity waves and by the time averaged value of the currents (e.g. undertow, longshore current). Consequently, these irregularities have an influence on the time scales of sand suspension and transport and make it difficult to compare with the results of laboratory experiments for monochromatic waves. Special measurements are necessary to study the processes of suspension and transport of sand under field conditions with a sampling rate frequency, which is much higher than the frequency of the surface waves. This is a difficult task, but it is the only possible way to obtain reliable data for the description of the physical processes. Those data are needed to invent suitable models for the calculation of sediment transport.

The mechanism and the time scale of sand suspension by irregular waves are considered in this paper on the basis of special field experiments.

Die Küste, 64 (2001), 161-200

2. Test sites

Synchronous field measurements have been carried out during the experiments "Novomichailovka'93" in the Black Sea, "Norderney'94" in the North Sea and "EbroDelta'96" in the Mediterranean Sea (PYKHOV et al., 1995; KUNZ and KOS'YAN, 1997; SANCHEZ-ARCHILLA et al., 1998). The locations of the testing sites for the field experiments are shown in Fig. 1. The programs of the experiments "Norderney'94" and "EbroDelta'96" have been diverse, universal and complicated. However, this paper is restricted to the measured data and related results, as far as they are connected with the aim of this paper. These measurement comprehend high frequency records of suspended sediments, water velocity, free surface elevation and erosion/accretion, as well as sampling of sediment in the water column and out of the bottom layer, observations of the bottom profiles and of the ripple structures.

The field experiment "Novomichailovka'93" was carried out on the barred beach near the Novomikhailovka settlement (Krasnodar region, Russia) on the Black Sea shore in De-

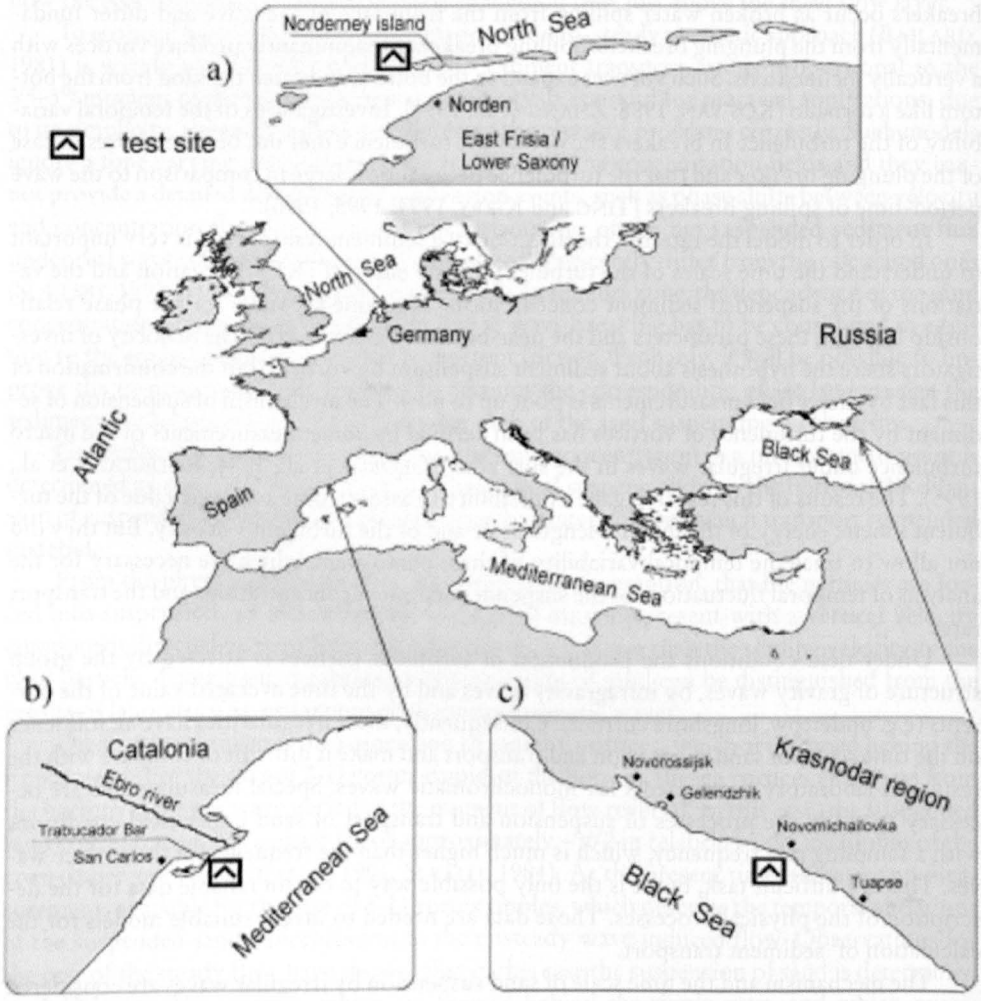

Fig. 1: Locations of the field experiments "Norderney'94"/Germany (a), "EbroDelta'96"/Spain (b), "Novomichailovka'93"/Russia (c)

cember 1993. The Black Sea is non-tidal. The measurements were adapted to wind waves and swell, and concentrated on one point located offshore the surf zone at a depth of 2.7 m. During the experiment the significant wave heights were up to 0.9 m and the periods reached 8.3 seconds.

The field experiment "Norderney'94" was performed on the non-barred western part of Norderney Island, North Sea (Germany), in October 1994. The mean tidal range is almost 2.5 m (high-meso tidal); the tide is lunar semidiurnal. Synchronous measurements of the suspended sediment concentration, the water velocity and the free surface elevation were carried out predominantly in the outer and middle parts of the surf zone (wind waves and swell) in two points of the bottom profile. The tidal range permitted measurements over a depth ranging from 0.4 m to 2.2 m. During the experiment the significant wave heights reached 1.8 m and the wave periods were up to 9 s.

The field experiment "EbroDelta'96 was carried out in the Trabucador bar of the Ebro Delta, The Mediterranean Sea (Spain), in November 1996. The sandy barred beach is longshore uniform. The classification related to the tidal range is micro-tidal. Measurements focused on the surf zone (from the shoreline into a depth of approximately two meters). During the experiment the significant waves were not higher than 0.6 m and the periods reached 7 seconds.

At the sites of the experiments the nearshore isobaths run parallel to the coastline. The mean diameter of the bottom sediments ranged from 0.21 to 0.24 mm. The bottom slopes in the measurement areas were about 1:40 to 1:100. The bottom profiles and the measurement points for the three experiments are shown by Fig. 2.

During the experiment "Novomichailovka '93" the gauges were installed on a trestle of 300 meter length; during the "Norderney '94" experiment they were fixed on piles which had been driven into the sand bottom (Fig. 3b); during the "EbroDelta'96" the devices had been mounted on a sledge which was moved in the cross-shore direction by ropes (Fig. 3a). The gauge data were recorded by computers on shore connected with the devices by cables.

3. Methods and devices

The suspended sand concentration, the three components of the water particle velocities and the free surface elevation (waves) were measured synchronously at each measurement point with a sampling rate of 5 Hz over one hour and/or 20 Hz over 20 minutes.

The 5 Hz-series were used for investigations of the process of sand suspension at the time scales of gravity waves, infragravity waves and wave groups. Typically, in our experiments the gravity wave frequency bands were 0.08 to 0.6 Hz; for the infragravity waves and the gravity waves groups the frequency bands were lower than 0.08 Hz. The 20 Hz-series were used to investigate the sand suspension process on time scales of turbulent fluctuations in the surf zone, which corresponded to frequencies of more than 0.8 Hz for the test field conditions.

During the experiments we tried to measure as many wave regimes as possible. In "Novomichailovka'93" only eleven of the 5 Hz-series were registered due to the short periods with storm conditions. During "Norderney'94" the main part of the most interesting results was received. Due to the tidal conditions the wave regime at the measuring points changed continuously and consequently covered a wide range of wave parameters. Luckily, two storm periods occurred during the experiment. Therefore it was possible to obtain 44 of the 5 Hz-series and 35 of the 20 Hz-series. During "EbroDelta'96" the waves were weaker than in the

Die Küste, 64 (2001), 161-200

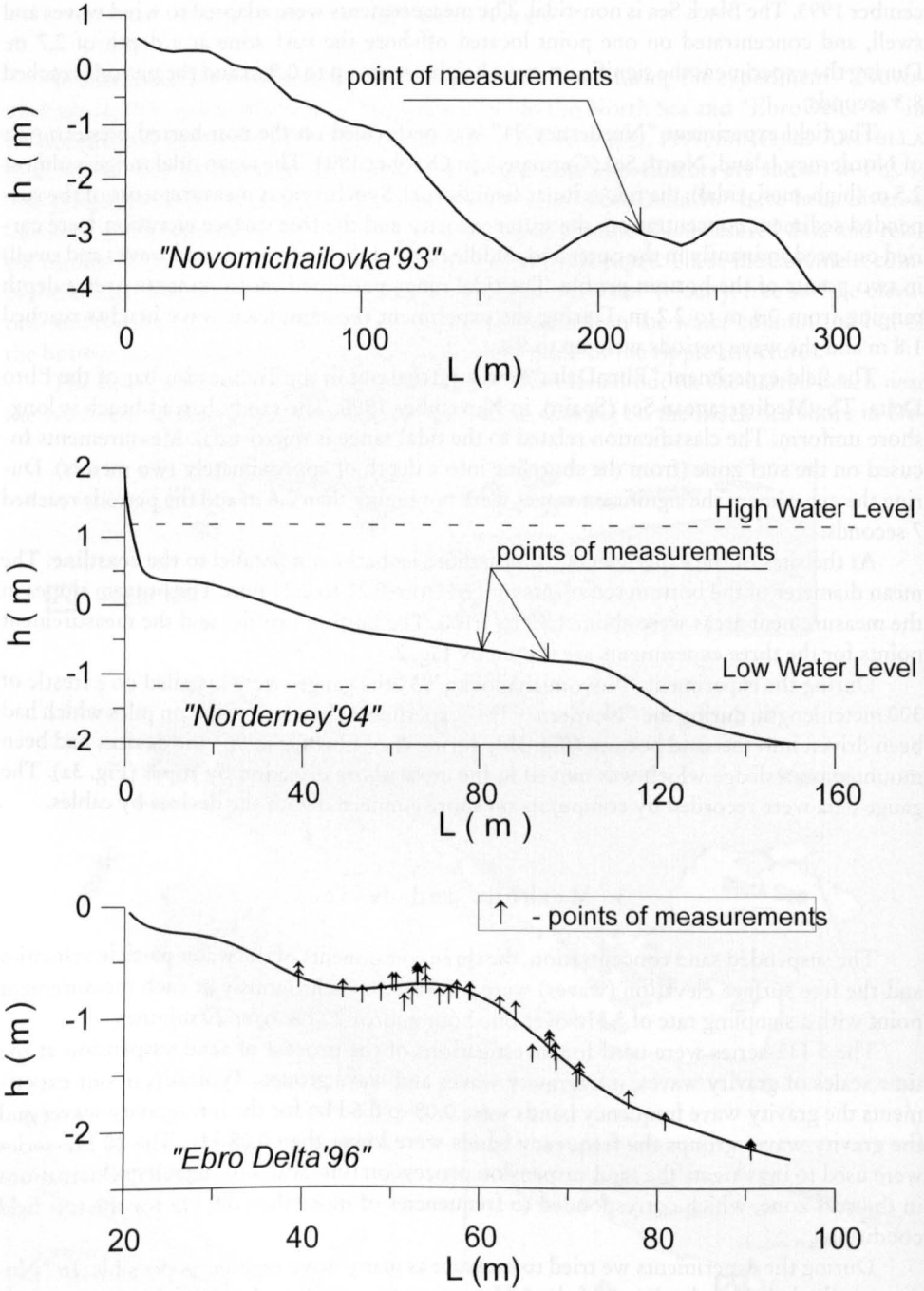

Fig. 2: Beach profiles and locations of the measurement points at the three field experimental sites

Die Küste, 64 (2001), 161-200

(a)

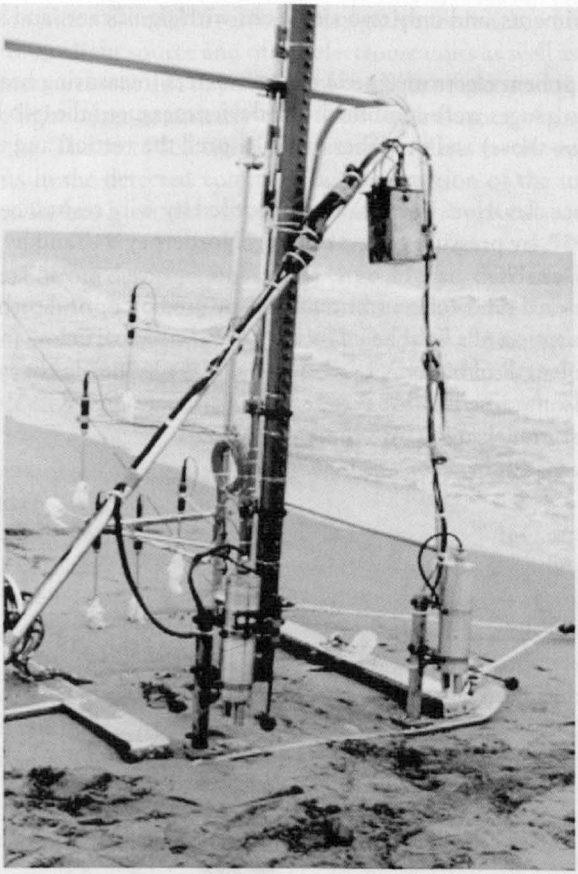

(b)

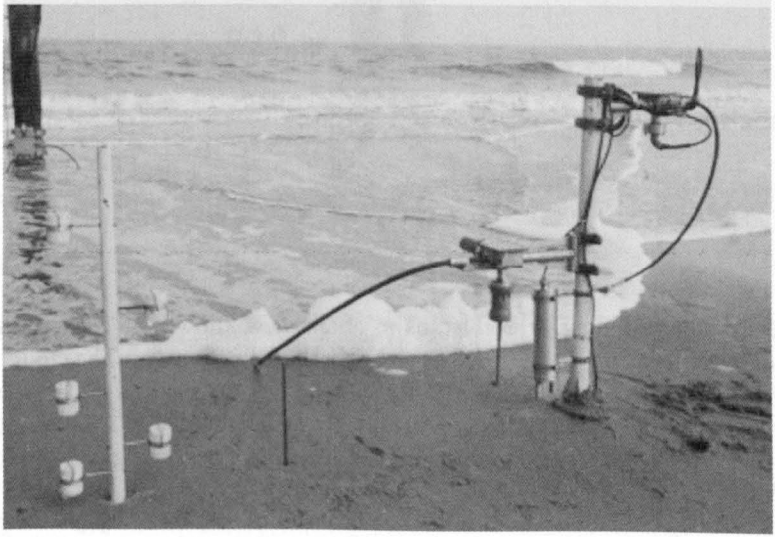

Fig. 3: View of sensors deployment used during the "EbroDelta'96" (a) and the "Norderney'94" experiment (b)

Die Küste, 64 (2001), 161-200

previous experiments, and only two situations with significant sand suspending events were recorded.

Two-component electromagnetic current meters (measuring heads of 60-mm diameter) were used. Two gauges were combined: one device measured the two horizontal components (long- and cross-shore) and the other one measured the vertical and the cross-shore component.

Free surface elevations (waves) were recorded by wire resistance gauges during "Novomichailovka '93", by pressure gauges during "Norderney'94" and by electric-contact gauges during "EbroDelta'96".

The suspended sand concentration was measured by optical turbidimeters, realizing the principle „absorption of a light beam by suspended solid particles" in the investigated water-column with a length of 60 mm (KOS'YAN et al., 1995). During the last years, the device has been constantly modified and it is patented in Russia now (KOS'YAN et al., 1999a). Fig. 4 shows the latest model of the turbidimeter.

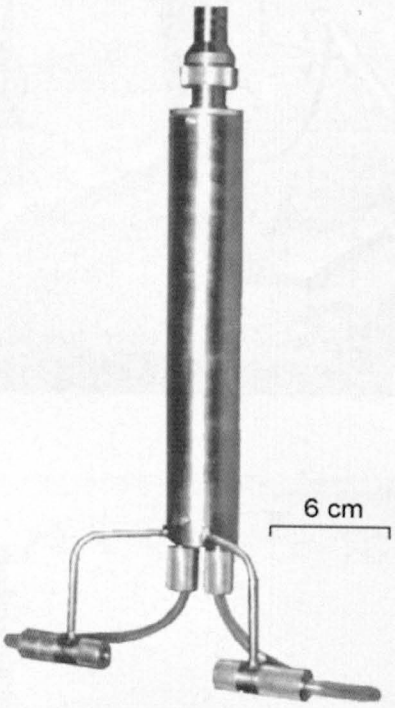

Fig. 4: The "Turbidimeter" – device

The use of the turbidimeter enabled us to obtain new knowledge concerning the mechanisms of the suspension of sediments. It works in the following way. The modulated light beam traverses the water volume and is partly absorbed by the suspended particles. The attenuation is detected by a photoreceiver. A diaphragm reduces the angle in which a light beam can reach the receiver. A precise photocurrent amplifier increases the signal from the photoreceiver. Afterwards it is demodulated, filtered and transferred as an analog signal to the registration device by communication cable. The electronic unit, which forms the registered signal, is working as a self-tuning loop with negative feedback, which ensures an independence from the cable resistance.

Die Küste, 64 (2001), 161-200

The turbidimeter contains a channel for an optical negative feedback, which removes the temperature instability of the light source and of the electronic units as well as the influences on the accuracy of the measurement due to an aging of the light source and the photoreceiver. The modulation of a light beam completely eliminates the influence of daylight on measurements in small depths. The recorded signal functionally relates to the concentration of the suspended sediments in the detected volume. The construction of the turbidimeter, its application and calibration has been described in more detail by KOS'YAN et al. (1995), KOS'YAN et al. (1999 b).

During a storm, the bottom deformations can be large. Hence, the distance between the sensors of a turbidimeter and the bottom surface should be adjustable. The time averaged concentration of the suspended sediment significantly depends on the distance from the bottom surface. Hence, the recorded data will vary considerably with the change of this distance. We used a special sand level gauge to control the distance between the sensors and the bottom (KOS'YAN et al., 1996; KOS'YAN and PODYMOV, 1997d). This device measures continuously the deformation of the bottom surface below the location of the sensor for the concentration measurement (KOS'YAN et al., 1997c).

Fig. 5 shows an example from the "Norderney'94" experiment during one of the storms. It visualizes oscillations of the bottom surface level during the measured time period of up to 14 cm. Further measurements which have been carried out in the same test field within the framework of field investigations for the improvement of artificial beach nourishment (KUNZ, 1999), showed storm induced bottom changes between consecutive tidal low-waters of more than one meter. This emphasizes, that a reliable information on the distance between the turbidimeter and the bottom surface is necessary for the interpretation of the recorded data and their final processing. The parameters which describe the bottom ripples were measured by scuba divers.

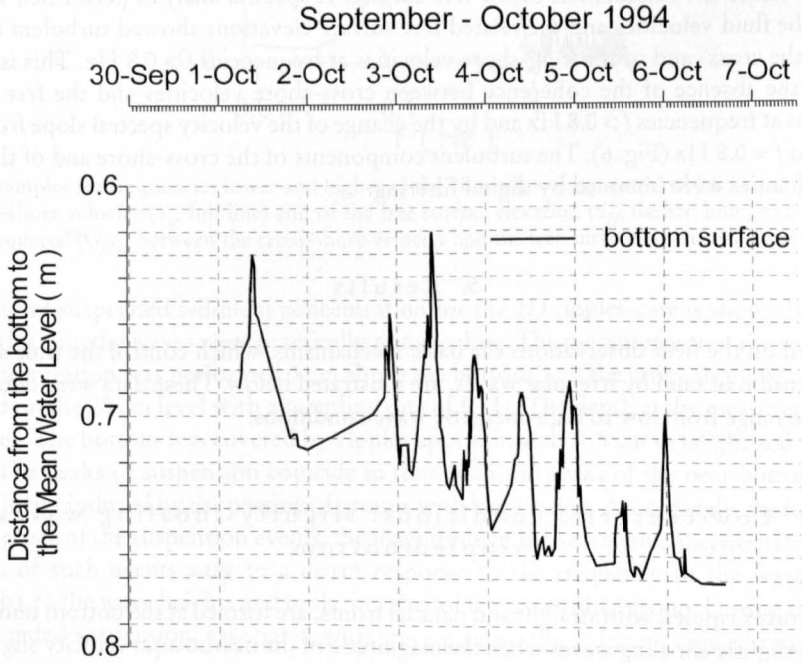

Fig. 5: Example for the change of the bottom surface over time measured by the Sand Level Gauge ("Norderney'94")

Die Küste, 64 (2001), 161-200

The turbidimeters were placed at a level between 5 to 25 cm, and the current meters at a level between 15 and 35 cm above the bottom. The horizontal distances between turbidimeters and current meters were 10 to 15 cm. More precise information on the positions of the devices can be drawn from the chapters referring to a description and discussion of the results.

4. Data processing

The existence of bottom ripples and their parameters for recording times during which scuba diving was impossible, was estimated by the formulae of NIELSEN (1991) and KOS'YAN and KOCHERGIN (1992) as well as by the diagram of KANEKO (1981).

The spectral analysis of time series was performed by applying the "Welch method" with a "Nuttal spectral window" – width of 0.01 Hz (MARPL,1987). The applied number of degrees of freedom was seventy.

The envelope for the fluctuations of the velocity which is induced by gravity waves ($u_e(t)$), was used to estimate the wave group structure. It has been calculated by the Hilbert transform method as:

$$u_e(t) = \left(\left\{\widetilde{L}\left(u(t)\right)\right\}^2 + \left(\widetilde{H}\left\{\widetilde{L}\left(u(t)\right)\right\}\right)^2\right)^{1/2} \qquad (1)$$

where $\widetilde{H}$ is the Hilbert transformation, $\widetilde{L}$ is a linear filtering operator that keeps only the frequencies of the gravity range, and $u(t)$ is the velocity of a water particle. Depending on the wave regime, the low frequency-boundary was especially determined by defining it as the beginning of a sharp rise of the spectral values; the upper boundary was fixed at 0.4 Hz.

The turbulence was considered as those parts of the water particle-velocity, which were not coherent to the fluctuations of the free surface. A spectral analysis performed with the data of the fluid velocities and the related free surface elevations showed turbulent fluctuations of the cross- and of the long-shore velocities at frequencies $f > 0.8$ Hz. This is confirmed by the absence of the coherence between cross-shore velocities and the free surface elevations at frequencies $f > 0.8$ Hz and by the change of the velocity spectral slope from $\sim f^{-4}$ to $\sim f^{-2}$ at $f = 0.8$ Hz (Fig. 6). The turbulent components of the cross-shore and of the long-shore velocities were obtained by digital filtering.

5. Results

Based on the field observations the basic mechanisms, which control the time scales of the suspension of sand by irregular waves, are illustrated below. These data were obtained in the whole range from low to high energetic wave conditions.

5.1 Low energetic conditions: slightly shoaling waves, rippled bottom

2D vortex ripples, with straight and parallel fronts, are formed at the bottom under non-breaking, slightly shoaling waves when the magnitude of the nearbottom velocity slightly exceeds the threshold value for the beginning of sand motion. The lee vortex ejection at the moment of flow reversal is the main mechanism of sand suspension. The example of temporal

Die Küste, 64 (2001), 161-200

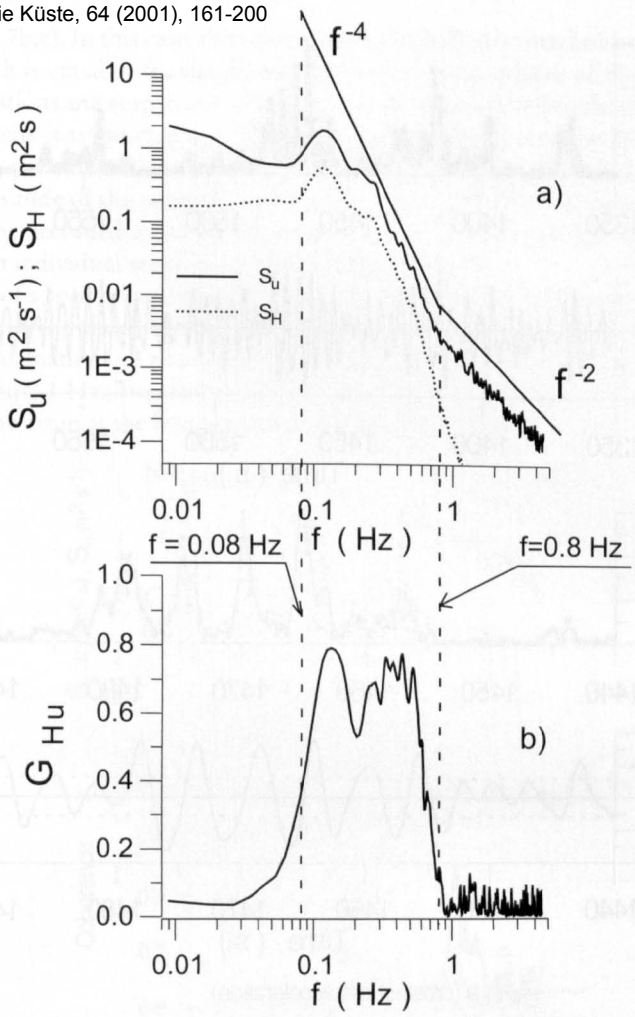

Fig. 6: Examples for frequencies lower and higher as the "boundary frequency" of 0.8 Hz: a) Spectra of the cross-shore velocity (S_u, full line) and of the free surface elevation (S_H, dashed line); b) Coherence squared (G_{Hu}) between the cross-shore velocity and the free surface elevation (waves)

variability of suspended sediment concentration for the 2D ripples-case is shown by Fig. 7. During this run, the waves were practically not shoaling. The measurement of the suspended sand concentration was performed 3 cm above the bottom, and the cross-shore velocity was recorded on the 25 cm level with a sampling rate of 5 Hz. The depth at the measurement site was 2.7 m. The bottom was covered by ripples approximately 1.5 cm in height and 10 cm in length. The peaks of suspension coincide in time with the peaks of the near-bottom cross-shore velocity induced by the passing of groups with large waves. Accordingly, the frequency of occurrence of the suspension events, the magnitude of the sediment concentration and the duration of such events vary in a direct response to the frequency of the wave groups (Fig. 7a,b), to the wave heights and to the number of waves within a group. During the events with extended suspension, associated with wave groups, the sediment concentrations fluctuated in response to the passing of individual waves within a group. For this run, the sand suspension began when a passing wave had induced a cross-shore velocity excluding a value

Die Küste, 64 (2001), 161-200

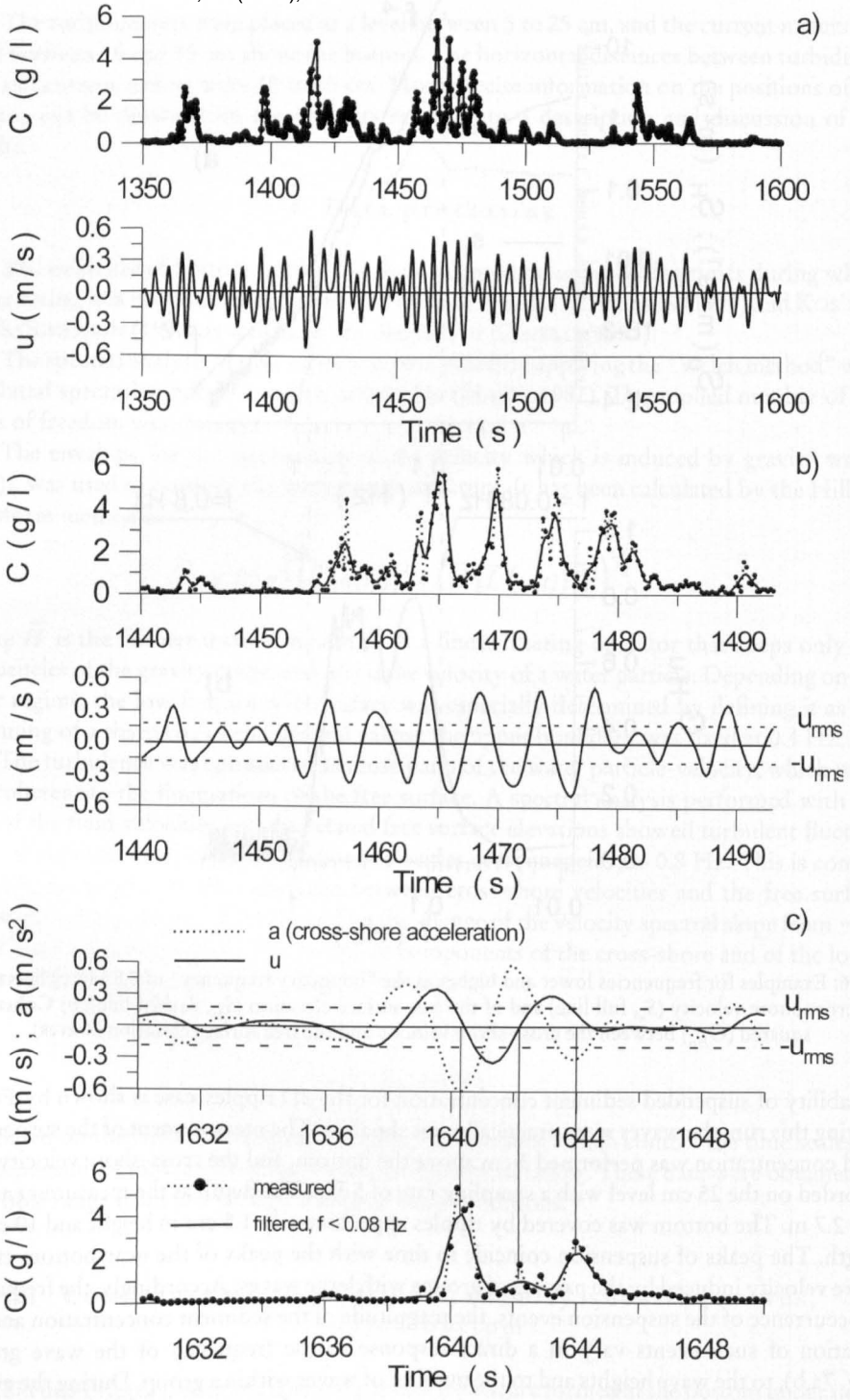

Fig. 7: Example for time series of the suspended sediment concentration (C) and the cross-shore velocity (u): a) passing of several groups with high waves; b) individual waves inside extended groups of high waves c) two large waves in the group ("Novomichailovka'93": H_s = 0.48 m; $T_{p=}$ 4.5 s; h = 2.7 m)

Die Küste, 64 (2001), 161-200

of 0.18 m/s (Fig. 7b,c). In this case, the value was almost 0.20 m/s (marked by dashed lines in Fig. 7 b,c), which is equal to the magnitude of the root-mean-square of the velocity (u_{rms}). No vortex formations and suspension of sand have been observed when the magnitude of the cross-shore velocity was less than u_{rms}. The peaks of the sediment concentration were mainly observed during the deceleration phase, with maxima at the moments of the flow reversal (maximum magnitude of the negative acceleration). During the flow acceleration phase, the magnitude of the recorded concentration peaks is significantly smaller and they do not appear with each individual wave in a group of high waves.

The results of a spectral analysis of the described time series are presented in Fig. 8. The spectrum of the cross-shore velocity (S_u) shows a local peak at a frequency of 0.2 Hz (Fig. 8a). The fluctuations of the velocity are smaller by one order of magnitude for frequencies less than 0.1 Hz. Two feebly marked local peaks characterize the suspended sand concentration spectrum at the frequencies of 0.2 Hz and 0.4 Hz.

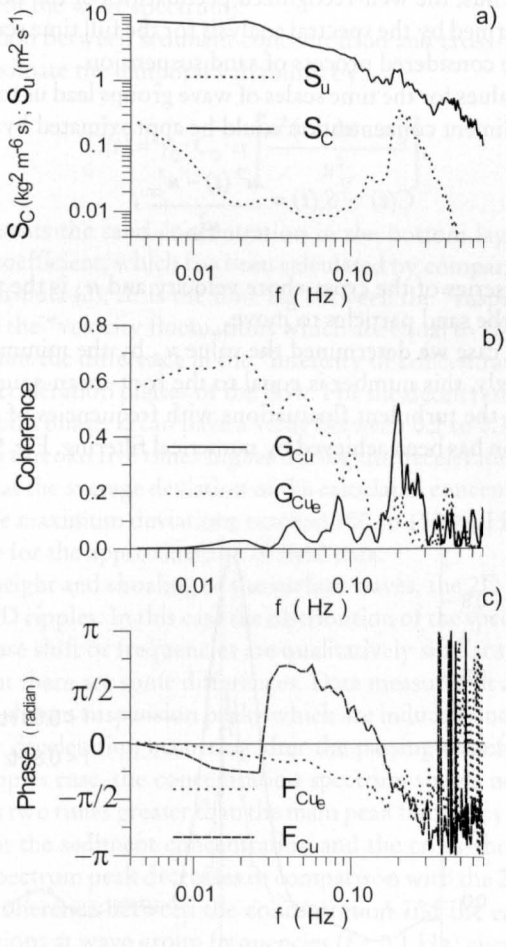

Fig. 8: Spectra, coherence and phase shift for Low Energetic Conditions: a) spectra of the suspended sediment concentration (S_C) and of the cross-shore velocity (S_u); b) coherence function between the sediment concentration and the cross-shore velocity (G_{Cu}); coherence function between the sediment concentration and the cross-shore velocity envelope (G_{Cue}); c) phase shift between the sediment concentration and the cross-shore velocity (F_{Cu}); phase shift between the sediment concentration and the cross-shore velocity envelope (F_{Cue})

Die Küste, 64 (2001), 161-200

The sediment concentration fluctuations are coherent with the cross-shore velocity fluctuations at the frequency of the wave spectrum peak (0.2 Hz), which is confirmed by a value of the coherence squared (G_{Cu}) of about 0.5 (Fig. 8b). The low values of the coherence between the sediment concentration and the cross-shore velocity fluctuations at the frequency 0.4 Hz ($G_{Cu} < 0.15$) can be explained by the absence of the velocity fluctuations at this frequency. High magnitudes of the coherence squared between the sediment concentration and the cross-shore velocity envelope ($G_{Cue} = 0.3$ up to 0.7) at frequencies less than 0.1 Hz indicate the influence of the wave group modulation amplitude on the suspended sand concentration. The phase lag of approximately $-\pi/2$ between the cross-shore velocity fluctuations and the sediment concentration (Fig. 8c) confirms, that the suspension events coincide with the moments of flow reversals, as expected, since the waves in this run had almost no higher harmonics. The phase lag between the suspended sand concentration and the fluctuation of the cross-shore velocity envelope at frequencies < 0.1 Hz changes from $-\pi/4$ to 0 when the frequency decreases. Thus, the well-recognized peculiarities of the time series, as presented in Fig. 7, are well confirmed by the spectral analysis for the full time series, and consequently they are typical for the considered process of sand suspension.

High coherence values for the time scales of wave groups lead us to assume, that the temporal variability of sediment concentration could be approximated by:

$$C(t) \sim S_r(t) = \frac{u^2(t) - u_{cr}^2}{u_{cr}^2}, \qquad (2)$$

where $u(t)$ is the time series of the cross-shore velocity and u_{cr} is the threshold value of the velocity which forces the sand particles to move.

In the considered case we determined the value u_{cr} by the minimum square method to be 0.18 m/s. Surprisingly, this number is equal to the root-mean-square value of the cross-shore velocities, when the turbulent fluctuations with frequencies of more than 0.8 Hz are excluded. The exclusion has been achieved by numerical filtering. Fig. 9 shows results for the

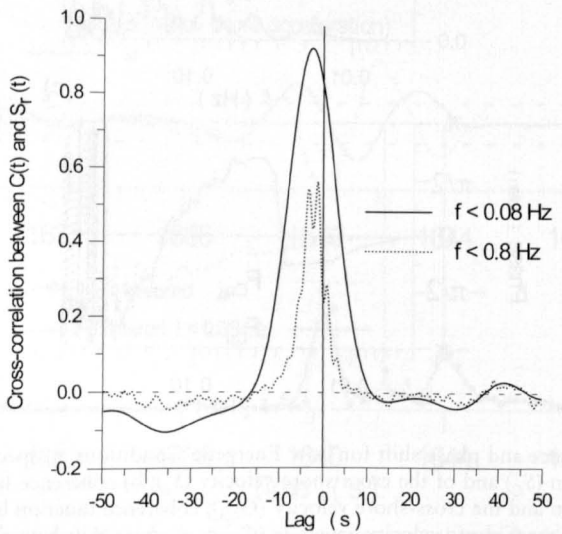

Fig. 9: Cross-correlation between $C(t)$ and $S_r(t)$ over lag for time series of the low frequency band ($f < 0.08$ Hz) and of the whole frequency band ($f < 0.8$ Hz) for the case of 2D ripples

cross-correlation between the measured sediment concentration $C(t)$ and the calculated values $S_r(t)$ for the distinguished bands of frequencies in dependency of the lag (time-shift between $C(t)$ and $S_r(t)$).

The solid line represents the change of the correlation coefficient for the frequency band of wave groups ($f < 0.08$ Hz) and the dashed line represents the frequency band below 0.8 Hz. The highest correlation between $C(t)$ and $S_r(t)$ with a value of approximately 0.9 is reached within the frequency band $f < 0.08$ Hz, when the measured fluctuation of the concentration differs about $\Delta t = 5$s from the calculated term $S_r(t)$. The maximum value of the correlation between the "fluctuation of concentration" and the $S_r(t)$ in the frequency band $f < 0.8$ is reduced (from 0.9 to 0.5) because the suspension of sediment by individual waves occurs only when $u(t) > u_{cr}$. The maxima for the correlation coefficients have been observed on time lag of 5 seconds (suspension caused by groups of high waves) and of 1.2 seconds (suspension by individual waves in groups). The time lag of 1.2 seconds corresponds approximately to T_p (T_p is the peak period of the wave spectrum).

The high correlation between sediment concentration and cross-shore velocity fluctuation permits to approximate the temporal variability by:

$$C(t) = \gamma_0 \cdot C_0 \cdot \alpha \left[\frac{u^2 (t - \Delta t - u_{cr}^2}{u_{cr}^2} \right], \qquad (3)$$

where $C_0 = 0.6$ represents the sand concentration in the bottom layer; $\gamma_0 = 8 \cdot 10^{-4}$ is the value of an empirical coefficient, which has been calculated by comparison of the gained field data with results of formula (3); Δt is the time lag between the "suspended sand concentration fluctuations" and the "velocity fluctuations which are equal to 1/4 T_p"; α is a coefficient which takes into account the difference in the "intensity of concentration peaks" during the deceleration and the acceleration phases of the flow. For the deceleration phase, α is equal to 1 and for the acceleration phase, α can have a value between 0.2 to 0.3 (the amplitude of the concentration peaks is three to five times higher during the deceleration phase). The investigations have shown that the average deviation of the calculated concentrations from the measured ones is 30 %; the maximum deviations reached 100 to 150 %. However, such an accuracy can be acceptable for the approximation of field data.

With increasing height and shoaling of the surface waves, the 2D ripples become unstable and transform to 3D ripples. In this case the distribution of the spectral density, of the coherence and of the phase shift or frequencies are qualitatively similar to the distributions for the 2D-ripple case. But there are some differences. Data measured at a distance of 3 to 7 cm from the bottom have shown suspension peaks which are induced once per wave period during the phase of flow deceleration occurring after the passing of deformed wave crests. In contrary to the 2D ripples case, the concentration spectrum shows no second local peak at the frequency which is two times greater than the main peak frequency of the wave spectrum. The phase lag between the sediment concentration and the cross-shore velocity at the frequency of the waves spectrum peak decreases in comparison with the 2D ripples case and has a value of $-\pi/3$. The coherence between the concentration and the envelope for the cross-shore velocity fluctuations at wave group frequencies ($f < 0.1$ Hz) also decreases to values of 0.3 to 0.45.

Because the waves were shoaling, the magnitudes of the cross-shore velocity under the wave crests were 1.5 to 2.0 times larger than those under the wave troughs. In this case, 3D ripples are not in equilibrium with the nearbottom velocities. By analogy to the data for non-equilibrium artificial 2D ripples (TUNSTALL and INMAN, 1975), it is possible to assume, that

Die Küste, 64 (2001), 161-200

in this case the formation of vortices and their ejection from the bottom begins earlier than in the case of the 2D ripples and of slightly shoaling waves.

In the case of 3D ripples, the maximum cross-correlation between the measured time series for the suspended sediment concentration and the parameter S_y is diminished by 30 % in comparison to the 2D ripple case, both for the whole frequency band and for the low-frequency range. The time lag is also reduced in comparison to the 2D ripples case and, accordingly, the phase shift between the concentration and the velocity changed from $-\pi/2$ (2D-case) to $-\pi/3$ (3D-case). Also in this case, the statistically significant values of the correlation testify to the possibility of using a formula similar to formula (3) for calculations of the temporary variability of suspended sand concentrations near the bottom (with adjusted coefficients γ_0, α and Δt). Input data for the cross-shore velocity can be provided by field measurements or may be assigned analytically.

5.2 High energetic conditions: shoaling, non-breaking waves over nearly flat bed

Under high energetic conditions, the sea bed becomes nearly flat and an intensive sediment movement takes place in an oscillatory bottom boundary layer, when shoaling, non-breaking waves provide conditions which are represented by a Shields parameter which exceeds the threshold value of 0.8. Typical examples for the temporal variability of suspended sand concentration and cross-shore velocity are shown on Fig. 10 and Fig. 11. The measurements of the concentration were performed 7 cm above the bottom, and the cross-shore velocity was recorded at the 25 cm-level. For both examples, it can be estimated that according to the method proposed by KANEKO (1981), there were 3D ripples at the bottom with a steepness of about 0.02 to 0.03, being in a state of erosion.

The in-depth visual analysis of a two hour record has shown that peaks of the concentration appear only after the wave crest has passed, and at the moment when the maximum values of the cross-shore velocity exceed 0.5 m/s. At those fragments of the time series, where the maximum values of the velocity are about 1 m/s, the concentration peak coincides with the middle of the flow deceleration phase (Fig. 10). At those fragments with cross-shore velocities of 0.5 to 0.8 m/s, the concentration peaks coincide with the flow reversal for the deceleration phase which occurs at the backside of waves (Fig. 11). The results of a spectral and a mutual spectral analysis for this run are presented on Fig. 12. The cross-shore velocities and the sediment concentration spectra show two local peaks at frequencies of appr. 0.12 Hz and appr. 0.25 Hz (Fig. 12a). For these frequencies this coherence shows a good correlation between the suspended sand concentration and the cross-shore velocity (Fig. 12b). The phase lag between these parameters at the frequency of the main spectrum peak (0.12 Hz) is nearly $-\pi/4$ (Fig. 12c).

The peculiarities of the peak appearance are mentioned above. The spectral analysis data correspond qualitatively with a hypothesis which explains the suspension of sand through turbulent vortices by an instability of the bottom boundary layer (FOSTER et al., 1994). This has been confirmed by describing the impact of wave induced turbulence on the bottom boundary layer (HINO et al., 1983; CONLEY and INMAN, 1992; COX and KOBAYASHI, 1999; 2000; NIHEI et al., 2000). According to the cited references, the turbulent kinetic energy has a maximum in the deceleration phase of a wave induced flow and decreases to zero immediately after the flow reversal. The inflection point of the curve for the cross-shore velocity is a necessary condition for shear instability, corresponding to the times of flow deceleration

Die Küste, 64 (2001), 161-200

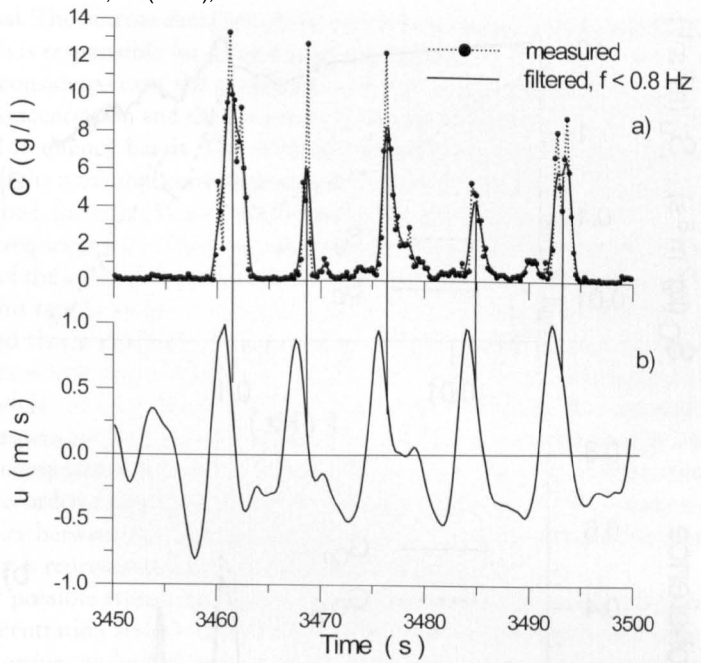

Fig. 10: Fragment (50 s) of the 5 Hz time series: a) for the suspended sand concentration (C) in the frequency range $f < 0{,}8$ Hz and for the range without turbulent fluctuations ($f < 0{,}08$ Hz); b) cross-shore velocity (u) in the case of nearly plane bed – "Novomichailovka'93": $H_s = 0.85$ m; $T_p = 8.3$ s; $h = 2.7$ m

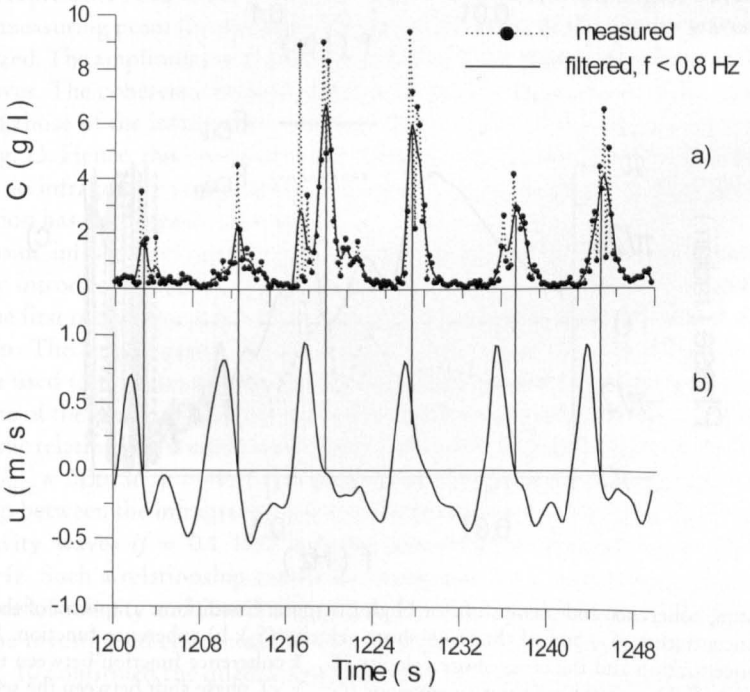

Fig. 11: Like Fig. 10, but for another fragment which represents the smaller amplitudes of the cross-shore velocity

Die Küste, 64 (2001), 161-200

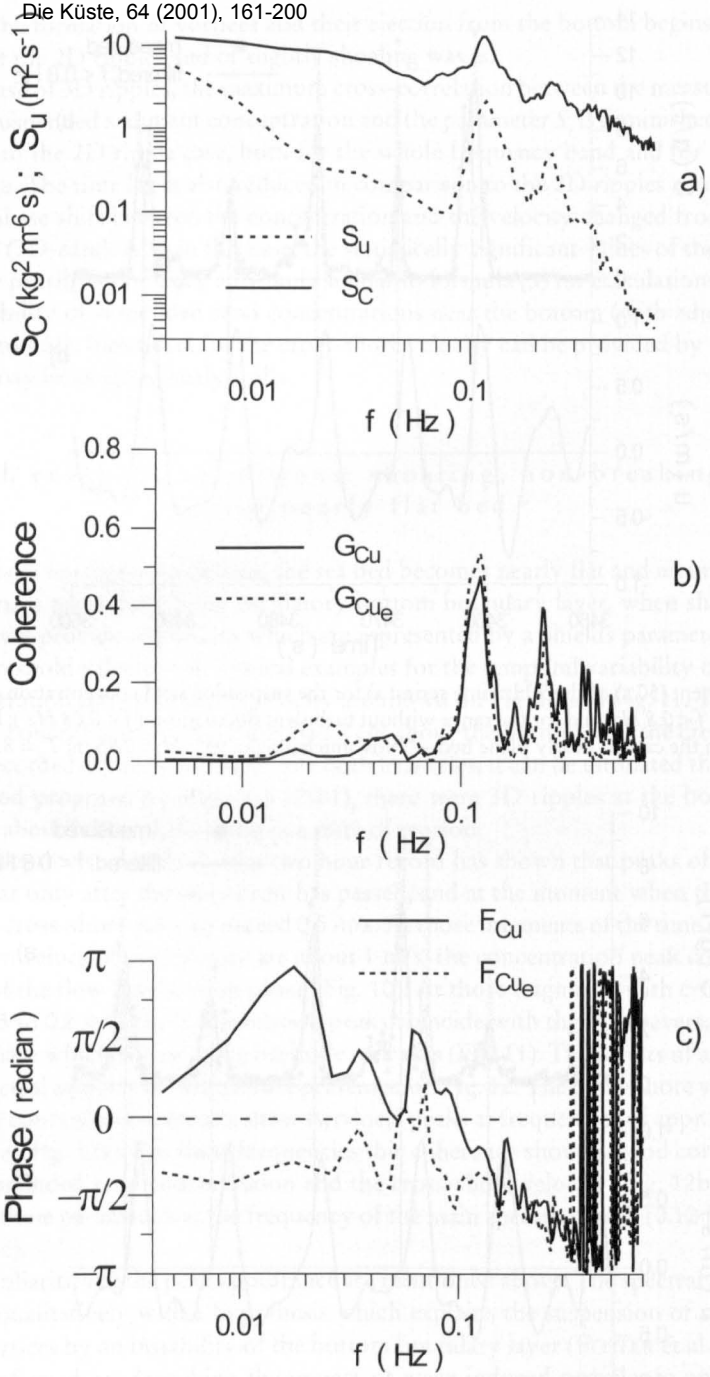

Fig. 12: Spectra, coherence and phase shift for High Energetic Conditions: a) spectra of the suspended sediment concentration (S_C) and of the cross-shore velocity (S_u); b) coherence function between the sediment concentration and the cross-shore velocity (G_{Cu}); coherence function between the sediment concentration and the cross-shore velocity envelope (G_{Cue}); c) phase shift between the sediment concentration and the cross-shore velocity (F_{Cu}); phase shift between the sediment concentration and the cross-shore velocity envelope (F_{Cue})

Die Küste, 64 (2001), 161-200
and its reversal. The bottom shear instabilities lead to an abrupt increase of the turbulence intensity, which is responsible for a rapid sand suspension.

For the considered case, the evaluation of the cross-correlation between the fluctuation of the sand concentration and the parameter S_r shows a maximum value of 0.35 at a lag time of -2 s for all frequency bands. The estimation has shown, that the differences between the calculated and the measured concentrations are between ± 50 % and ± 300 %. Hence, for the case of a flat bed, formula (3) can only be applied as a rough estimation.

At low frequencies ($f < 0.08$ Hz) the concentrations are almost not coherent with both, fluctuations of the cross-shore velocity and their envelope (Fig. 12b). There are two possible reasons for this result. At first, the small magnitude of the coherence between the sand concentration and the cross-shore velocity or its envelope could be the effect of three-dimensional vortices which move with their central or circumferential part through the measurement point while carrying suspended sand. The effect would be, that the measured magnitude of the suspension peaks could substantially differ, although the velocity under the wave crests of the compared events is approximately the same. This can well be recognized from parts of the recorded time series, as shown on Fig. 10 and Fig. 11. The absence of a rigorous proportionality between the maximum values of the concentration and the maximum of the water velocity is represented by the low values of coherence.

Another possible reason for the small values of coherence at low frequencies between the sand concentration and the cross-shore velocity or its envelope is the joint influence of gravity wave groups and of infragravity waves on the process of sand suspension. Fig. 13 presents a 10-minute window of a time series for the concentration and velocity, which are typical for the high-energetic condition, as shown above by the Figs. 10 to12. These figures also present the gravity (u_g) – and the infragravity (u_i) – components of the velocity (u). The displayed run represents swell with $H_s = 0.85$ m, and $T_p = 8.5$ s. Only the largest waves have broken at the measuring point (by spilling). The group structure of the gravity waves can easily be recognized. The amplitudes of the infragravity waves are about half as large as those of the gravity waves. The coherence between the low-frequency fluctuations of the sand concentration and those of the infragravity waves as well as those of the wave groups are not obvious in Fig. 13. Hence, this case is contrary to the discussed case of the low-energetic waves, which has no infragravity components (Fig. 7) and where the effect of wave groups on the concentration has been clearly observed.

The joint influence of gravity and infragravity waves on the concentration can be checked by introducing a relationship between the velocity and the concentration of a higher than the first order. The coherence function is the estimate of the validity of a first order relationship. The results gained by applying a bicoherence function (G_{uuc}), as shown in Fig. 14, are used to estimate the quadratic relationship between two harmonics of the velocity and one of the concentration for the series which are presented in Fig. 13. The existence of a quadratic relationship is confirmed by the sufficiently high magnitude of the bicoherence function $G_{uuc} = 0.35$ at $f_1 = -0.1$, $f_2 = 0.015$ Hz. This example demonstrates a quadratic relationship between the infragravity wave at the frequency $f = 0.015$ Hz, the first harmonic of the gravity waves ($f = 0.1$ Hz) and the concentration fluctuation at the frequency $f = 0.085$ Hz. Such a relationship cannot be recognized by a simple view on synchronous chronograms of velocity and concentration and this may be the reason of the low coherence between the investigated concentration and velocity. The bicoherence function with input data of Fig. 10 confirmed the quadratic relationship between the first two harmonics of the velocity and the concentration fluctuation at the frequency of the first harmonic ($G_{uuc} = 0.35$ at $f_1 = -0.24$ Hz, $f_2 = 0.12$ Hz). The last result corresponds to the fact, that due to the sharp

Die Küste, 64 (2001), 161-200

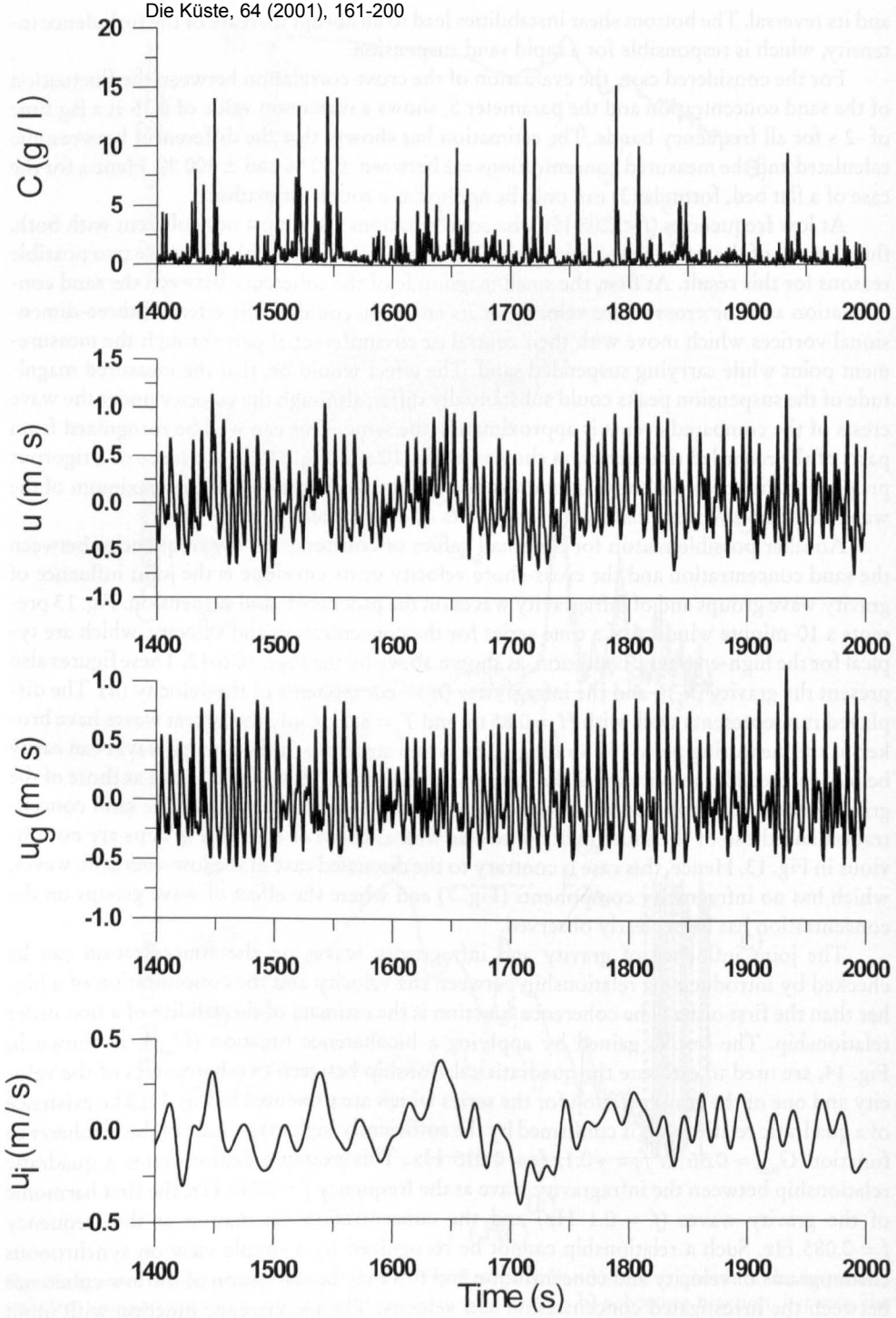

Fig. 13: Fragment of time series (600 seconds) of the sediment concentration (C), of the cross-shore velocity (u) with its gravity component (u_g) and its infragravity component (u_i) - "Novomichailovka'93": see Fig. 10

Die Küste, 64 (2001), 161-200

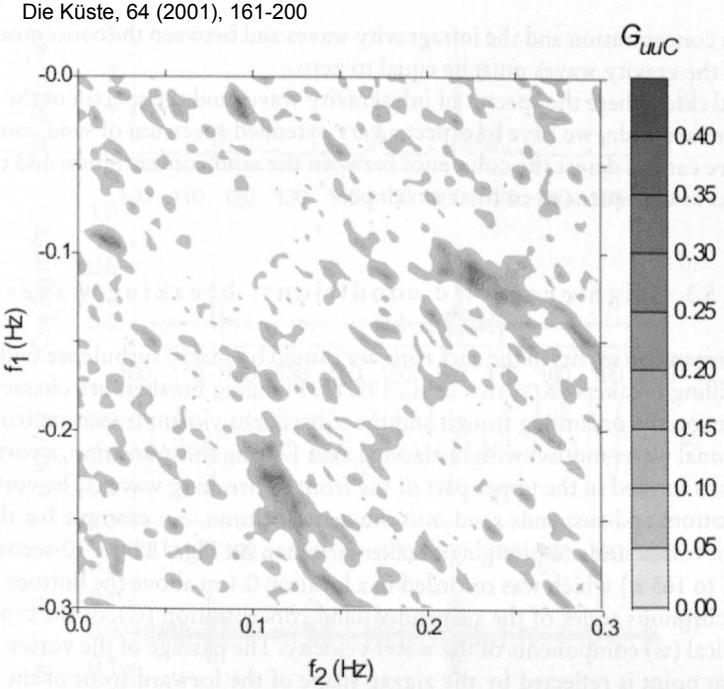

Fig. 14: Contours for the value of the cross bicoherene function (G_{uuC}) for two harmonics of the cross-shore velocity (f_1, f_2) and the suspended sediment concentration. Time fragment and input data: see Fig. 13

and high crest of the waves and the shallow and plain wave trough the concentration peak occurs only once per wave period.

A simple analytical model has been applied to investigate quadratic relationships. We can expect, similar to formula (3), a dependency of the sand concentration from the velocity: $C = Au^2$ with $A = constant$; u shall include the infragravity waves and the groups of gravity waves in the simplest form as

$$u(t) = cos(\omega_i t) + cos(\omega_{g1} t) + cos(\omega_{g2} t), \tag{4}$$

where the index i corresponds to the infragravity waves, $g1$ and $g2$ to the harmonics of the gravity waves; t is the time and w is the angular frequency.

The harmonics $g1$ and $g2$ produce the group structure of waves as

$$u_g = cos(\omega_{g1} t) + cos(\omega_{g2} t) = cos(\omega_e t)\, cos(\omega_g t), \tag{5}$$

where $w_e = (\omega_{g1} - \omega_{g2})/2$ is the frequency of the envelope and $\omega_g = (\omega_{g1} + \omega_{g2})/2$ is the main frequency of the gravity waves. As result we find, that

$$C(t) = A\{1.5 + 0.5\, cos(2\omega_i t) + 0.5\, cos(2\omega_{g1} t) + 0.5\, cos(2\omega_{g2} t) + cos[(\omega_i + \omega_{g1})t] + cos[(w_i - \omega_{g1})t] + cos[(\omega_i + \omega_{g2})t] + cos[(\omega_i - \omega_{g2})t] + cos[(\omega_{g1} + \omega_{g2})t] + cos[(\omega_{g1} - \omega_{g2})t]\}. \tag{6}$$

Among these eighth harmonics of concentration (6) there is neither the frequency of infragravity waves nor that of gravity waves. Therefore, in our simple model, the coherence

Die Küste, 64 (2001), 161-200

between the concentration and the infragravity waves and between the concentration and the envelope of the gravity waves must be equal to zero.

In a real case, where the spectra of infragravity waves and the spectra of the envelope of gravity waves are wide, we have to expect a very extended spectrum of sand concentrations, and therefore cannot detect the coherence between the sand concentration and the infragravity waves at low frequencies or their envelope.

5.3 High energetic conditions: breaking waves

Sand suspension events in the surf zone are caused by macro turbulence under the plunging and spilling breakers (KOS'YAN et al., 1997b). Plunging breakers are characterized by a jet impinging on the oncoming trough and the subsequent violent transition from irrotational to rotational water motion with horizontal axis. During this transition, a vortex with horizontal axis is formed in the upper part of the front of breaking waves. The vortex penetrates to the bottom and suspends sand into the water column. An example for the sand suspension by a vortex under a plunging breaker is shown on Fig. 15 by a 10-seconds segment (from 155 s. to 165 s.) which was recorded in a location 0.1 m above the bottom. The figures display synchronous series of the suspended sand concentration (C), of the cross-shore (u) and the vertical (w) components of the water velocity. The passage of the vortex through the measurement point is reflected by the zigzag shape of the forward front of the cross-shore

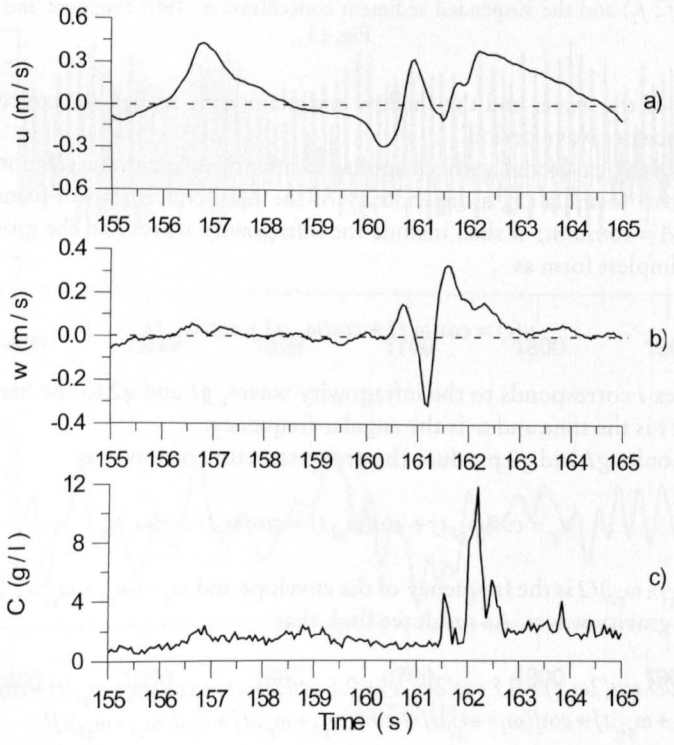

Fig. 15: Example for the high resolution of the record (time fragment of 10 seconds) for a sand suspension event (level 10 cm above the bottom) under a plunging breaker – "EbroDelta'96" experiment: a) cross-shore velocity (u); b) vertical velocity (w); c) suspended sediment concentration (C)

Die Küste, 64 (2001), 161-200

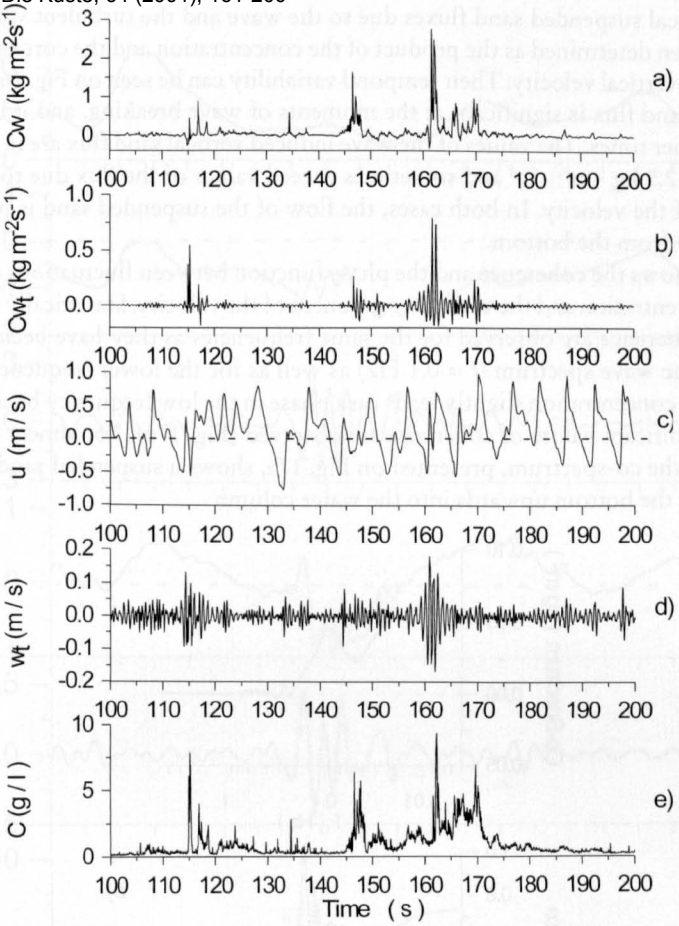

Fig. 16: Example (time fragment of 100 seconds) for the seaward part of the surf zone (10 cm above the bottom) under the conditions of plunging waves. – "EbroDelta'96" experiment: H_s = 0.4 m; T_p = 10 s; h = 0.5 m: a) vertical component of the suspended sand flux induced by the velocity of the wave component (Cw); b) vertical component of the suspended sand flux induced by the turbulent velocity (Cw_t); c) cross-shore velocity (u); d) vertical turbulent velocity (w_t); e) suspended sediment concentration (C)

velocity (Fig. 15a) and by the alternating changing of the direction of the vertical velocity component (Fig. 15b) during the time interval from second 160.5 to 162.5. The recorded character of the cross-shore and of the vertical velocity graphs is determined by a rotation of the vortex in the clockwise direction. The sand suspension event is related to the positive value of the vertical component of the vortex velocity, and it has some time lag with regard to the maximum of the vertical velocity.

The data presented in Fig. 15 confirm the fact, that the vertical velocity determines the suspended sand flux from the bottom. More obviously, it is illustrated by the data of the measurements which are shown in Fig. 16. The vertical velocity has been divided into the wave component (f < 0.8 Hz) and the turbulent component (f > 0.8 Hz) by digital filtering. The peaks of the concentration (Fig. 16e) coincide in time with the increased magnitudes of the turbulent fluctuations of the vertical velocity (Fig. 16d) and the zigzag form of the forward front of the cross-shore velocity (Fig. 16c).

Die Küste, 64 (2001), 161-200

The vertical suspended sand fluxes due to the wave and the turbulent velocity components have been determined as the product of the concentration and the corresponding component of the vertical velocity. Their temporal variability can be seen on Fig. 16a and Fig.16b. The vertical sand flux is significant at the moments of wave breaking, and it is insignificant during the other times. The values of the wave induced vertical sand flux are in the range between 0.7 and 2.5 $kg \cdot m^{-2} \cdot s^{-1}$ and sometimes exceed values of the flux due to the turbulent component of the velocity. In both cases, the flow of the suspended sand is predominantly directed away from the bottom.

Fig. 17 shows the coherence and the phase function between fluctuations of the suspended sand concentration and the vertical component of the velocity. Statistically significant values of the coherence are observed for the same frequencies as they have been evaluated for the peak of the wave spectrum (f = 0.1 Hz) as well as for the lower frequencies (Fig. 17b). The sediment concentration slightly leads on a phase in the low frequency band (f < 0.1 Hz), where the significant values of coherence are observed (Fig. 17c). For almost the entire frequency band the co-spectrum, presented on Fig. 17a, shows a suspended sand flux which is directed from the bottom upwards into the water column.

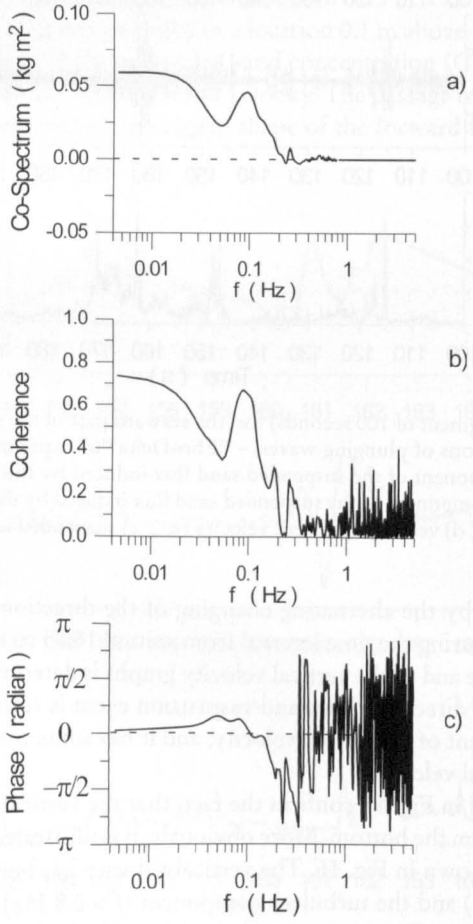

Fig. 17: Co-spectrum (a), Coherence (b) and Phase shift (c) between the suspended sand concentration (C) and the wave-induced component of the vertical velocity (Wt) for the time series data as displayed on Fig. 16

Die Küste, 64 (2001), 161-200

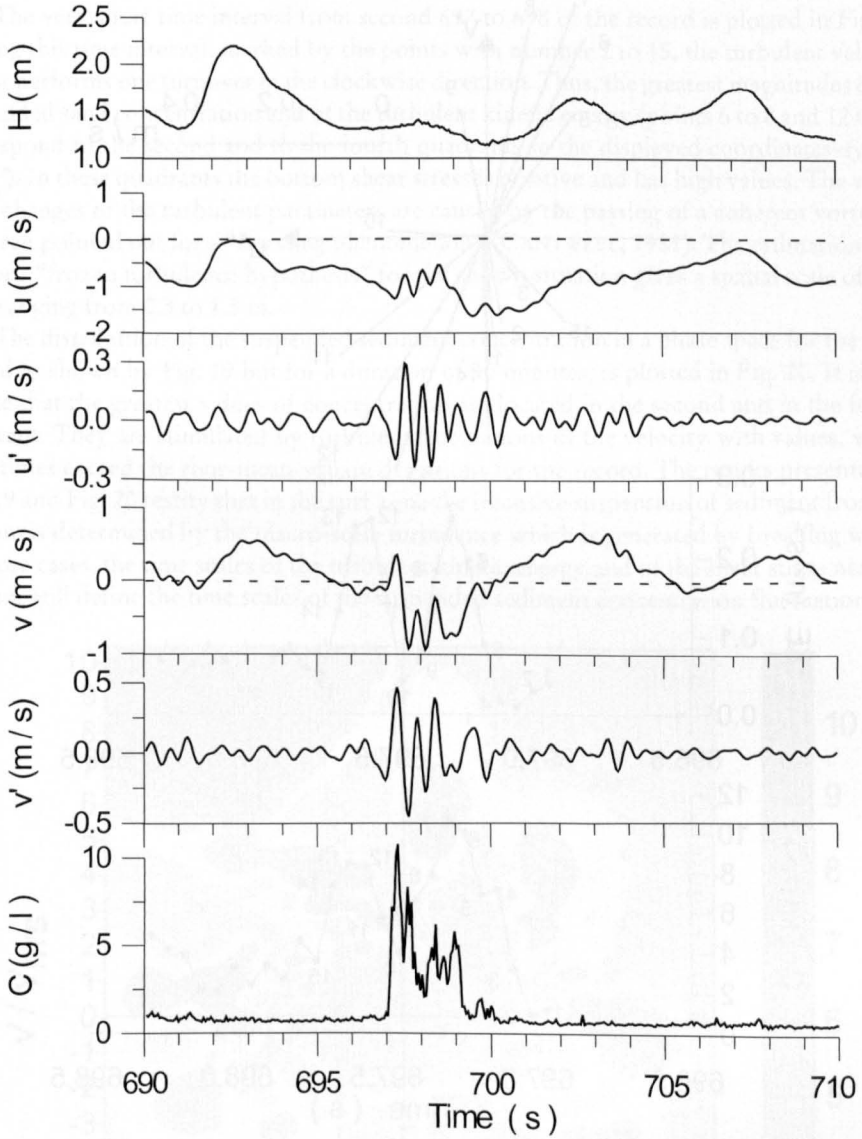

Fig. 18: Example (time fragment of 20 seconds) for a suspension event in the middle part of the surf zone under the conditions of spilling waves: suspended sediment concentration (C) in a distance of 10 cm and fluid velocities (u, u', v, v') in a distance of 15 cm above a flat bottom. – "Norderney'94" experiment: $H_s = 1.07$ m; $T_p = 8.7$ s; $h = 1.53$ m

During our measurements, wave breaking by spilling generally occurred inside the surf zone. An example for sand suspension by macro turbulent vortices in the middle part of the surf zone is shown in Fig. 18. A suspension event with a nearly vertical front coincides well with strong fluctuations of the cross-shore and of the long-shore velocity components in the time interval 697 to 700 second. Such very intensive turbulent fluctuations of the horizontal velocity component and of the suspension events are caused by vortices which pass directly through the measuring point.

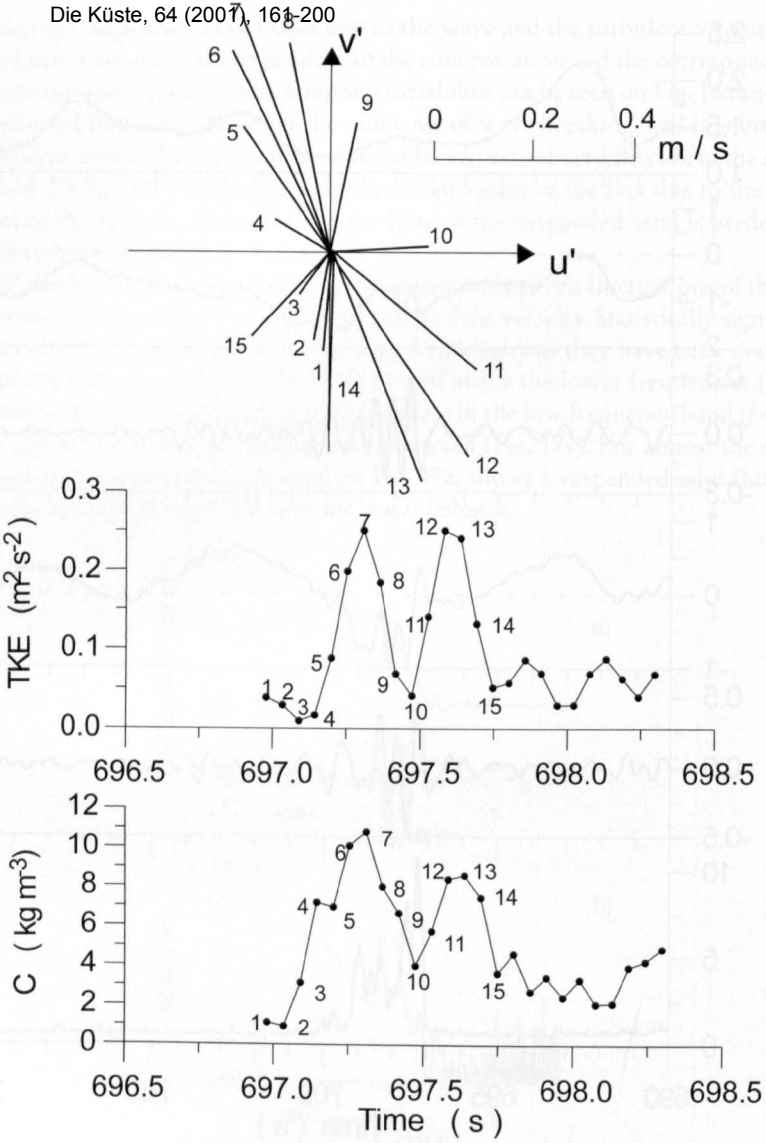

Fig. 19: Example for an extremely short fragment (time interval of 2 seconds) of the temporal variability of the sediment concentration (C), the 2D turbulent kinetic energy (*TKE*) and the position of the turbulent velocity vector (upper part of the Figure). The suspension event is shown on Fig. 18

A further confirmation, that the described suspension events are stimulated by vortices, can be drawn from the data which are shown in Fig. 19. The figure displays the time histories of the suspended sand concentration of the 2D turbulent kinetic energy (E) and an instantaneous vector, indicating the position of the turbulent velocity within the phase space.

$$E = 1/2(u'^2 + v'^2), \qquad (7)$$

where u' and v' are cross-shore and longshore turbulent velocities.

Die Küste, 64 (2001), 161-200

The very short time interval from second 697 to 698 of the record is plotted in Fig. 18. During this time interval, marked by the points with number 1 to 15, the turbulent velocity vector performs one turnover in the clockwise direction. Thus, the greatest magnitudes of the suspended sand concentration and of the turbulent kinetic energy (points 6 to 8 and 12 to 13) correspond to the second and to the fourth quadrants in the displayed coordinates-system (u', v'). In these quadrants the bottom shear stress is positive and has high values. The visualized changes of the turbulent parameters are caused by the passing of a coherent vortex, as has been pointed out for a "bursting phenomenon" (CANTWELL, 1981). The estimation with Taylor's "frozen turbulence hypothesis" for the shown situation gives a spatial scale of vortices ranging from 0.3 to 1.5 m.

The distribution of the suspended sediment concentration in a phase space for the same record as shown by Fig. 19 but for a duration of 30 minutes, is plotted in Fig. 20. It is well visible that the greatest values of concentration are located in the second and in the fourth quadrant. They are stimulated by turbulent fluctuations of the velocity with values, which sometimes exceed the root-mean-square deviations for the record. The results presented on Fig. 19 and Fig. 20 testify that in the surf zone the intensive suspension of sediment from the bottom is determined by the macro-scale turbulence which is generated by breaking waves. In those cases, the time scales of the turbulent kinetic energy and of the shear stress near the bottom will define the time scales of the suspended sediment concentration fluctuations.

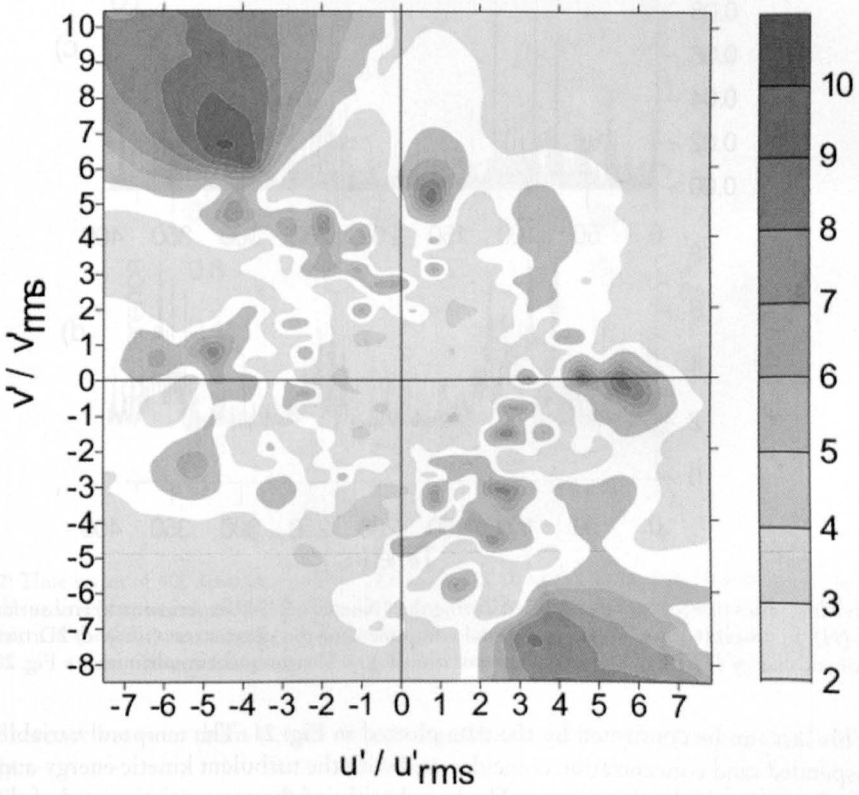

Fig. 20: Suspended sediment concentration plotted in the velocity space (u, v): u' and v' are the cross-shore and the longshore turbulent velocities; u'_{rms} and v'_{rms} are root-mean-square values of u' and v' – "Norderney'94" experiment: $H_s = 0.90$ m; $T_p = 8.7$ s; $h = 1.62$ m. Measurement points: 10 cm (sediment concentration) and 15 cm (velocities) above a flat bottom. Data: see Fig. 21

Die Küste, 64 (2001), 161-200

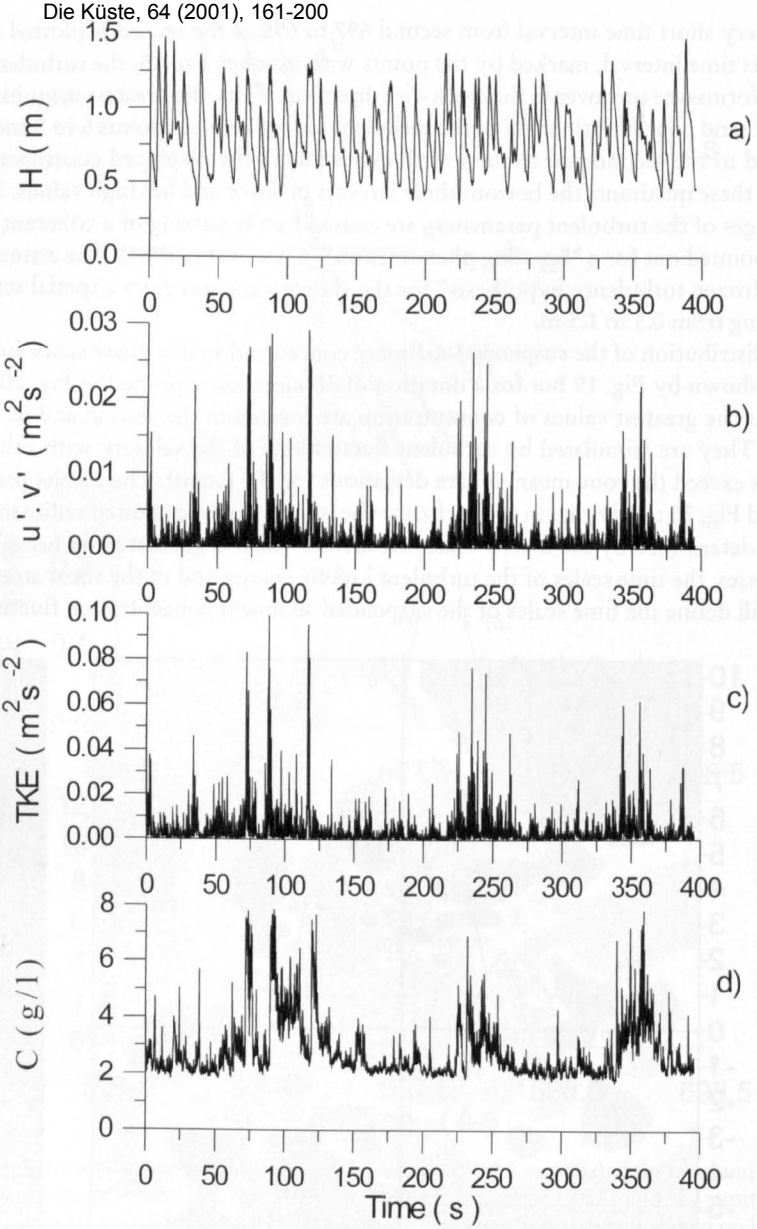

Fig. 21: Time series of 400 seconds recorded during the "Norderney'94" experiment: a) free surface elevation (*H*); b) absolute value of the horizontal component of the shear stress (*u'v'*); c) 2D turbulent kinetic energy (*TKE*); d) sediment concentration(*C*). – Measurement conditions: see Fig. 20

This fact can be confirmed by the data plotted in Fig. 21. The temporal variability of the suspended sand concentration coincides well with the turbulent kinetic energy and with the absolute value of the shear stress. The broad peaks of the concentration and of the turbulent kinetic energy follow with a periodicity between 100 s to 150 s. Inside such peaks, the fluctuations of these parameters on time scales of about the wave period were observed. Fig. 22 presents spectra of the cross-shore velocity, the suspended sand concentration and

Die Küste, 64 (2001), 161-200

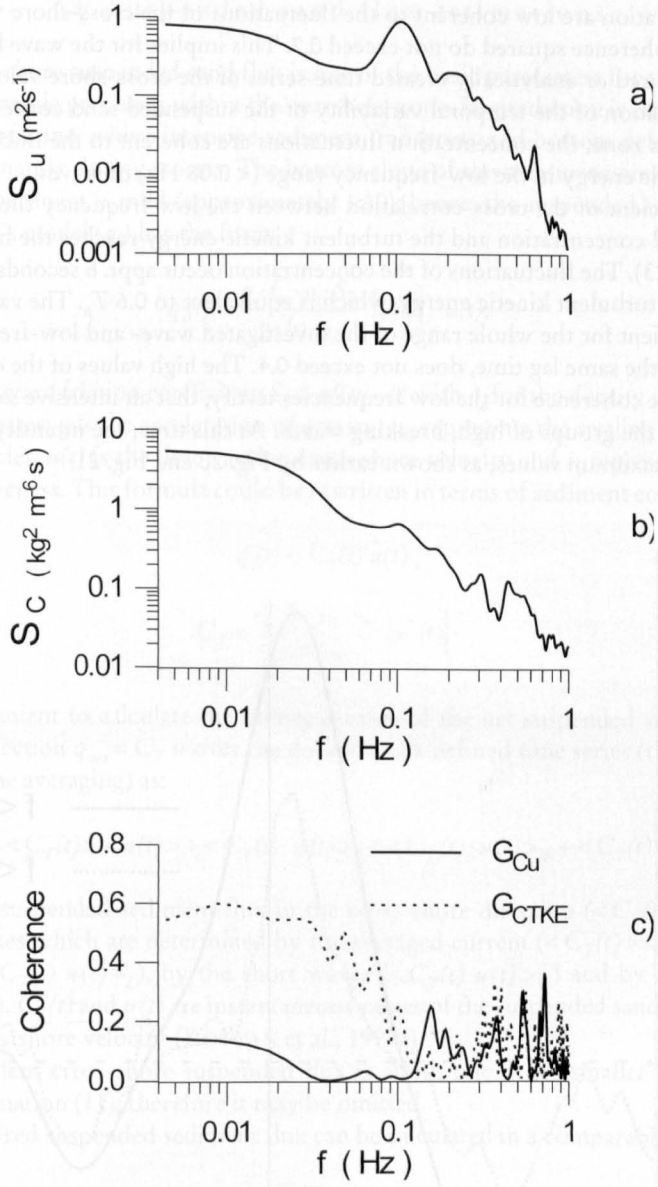

Fig. 22: Time series of 400 seconds (see Fig. 21): a) spectra *Su* of the cross-shore velocity (*u*); b) spectra *Sc* of the sediment concentration (*C*); c) spectra of the coherence between *Sc* and *Su* (G_{cu}) and between the spectra of the sediment concentration and of the turbulent kinetic energy (*Gctke*). – "Norderney'94" experiment, middle part of the surf zone; measurement conditions see Fig. 20

the coherence between them as well as between the concentration and the turbulent kinetic energy.

The spectrum of the cross-shore velocity has a distinct local maximum on the frequency of 0.1 Hz. In the spectrum of the concentration we practically do not detect such a local peak; the spectral density increases quasi-monotonously with decreasing values of the frequency. In the range of the gravity and of the infragravity frequencies ($f < 0.8$ Hz), the fluctuations

Die Küste, 64 (2001), 161-200

of the concentration are low coherent to the fluctuations of the cross-shore velocity, as the values of the coherence squared do not exceed 0.2. This implies for the wave breaking zone, based on measured or analytically created time-series of the cross-shore velocity, that a reliable determination of the temporal variability of the suspended sand concentration is impossible. In this zone, the concentration fluctuations are coherent to the fluctuations of the turbulent kinetic energy in the low-frequency range (< 0.08 Hz) of waves.

The coefficient of the cross-correlation between the low-frequency time series of the suspended sand concentration and the turbulent kinetic energy reaches the highest value at appr. 0.7 (Fig. 23). The fluctuations of the concentration occur appr. 6 seconds after the fluctuations of the turbulent kinetic energy, which is equivalent to 0.6 T_p. The value of the correlation coefficient for the whole range of the investigated wave- and low-frequencies, with approximately the same lag time, does not exceed 0.4. The high values of the correlation coefficient and the coherence for the low frequencies testify, that an intensive sand suspension happens under the groups of high, breaking waves. At this time, the intensity of the turbulence reaches maximum values, as shown earlier by Fig. 20 and Fig. 21.

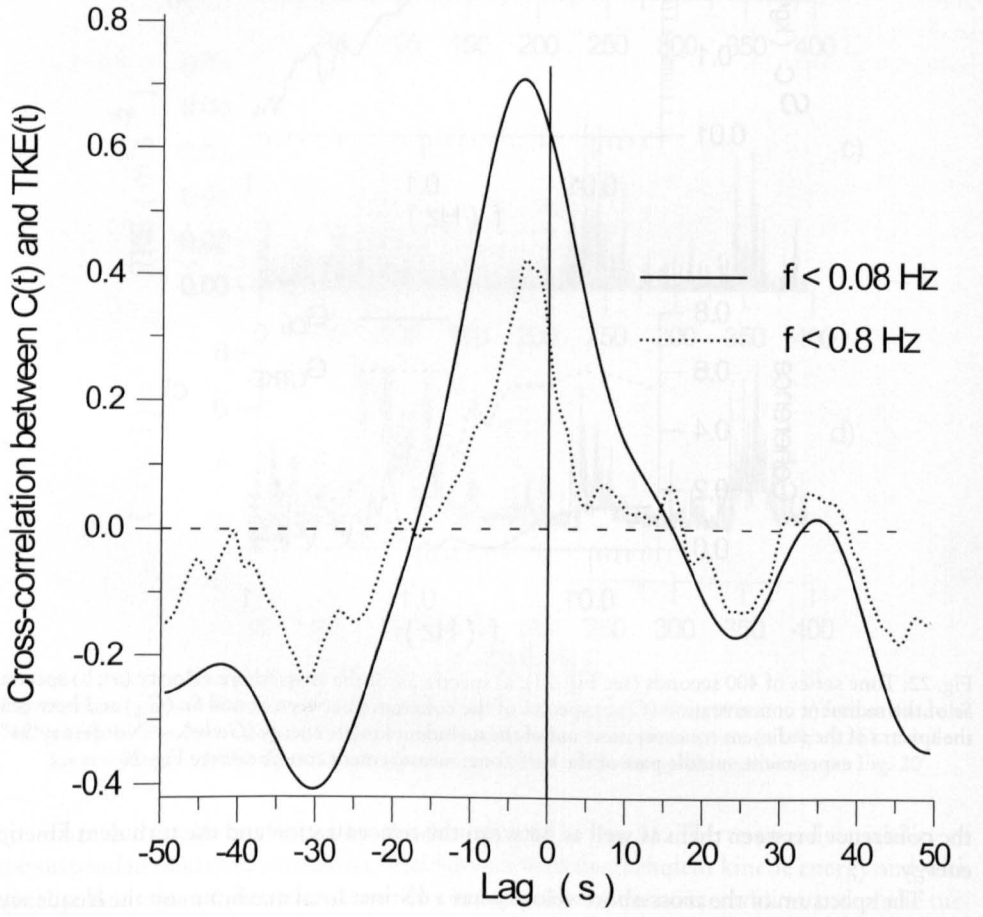

Fig. 23: Cross-correlation (*Cr*) between the suspended sediment concentration (*C(t)*) and the turbulent kinetic energy (*TKE*) for two frequency bands (*f*). Measurement conditions and data of the time series: see Fig. 20 and Fig. 21

Die Küste, 64 (2001), 161-200

5.4 Suspended sand flux estimations

The cross-shore suspended sand flux is one of the basic parameters for the modeling of the morphodynamic processes within the nearshore zone. Its prediction is especially important for the surf zone, where intensive sediment transports and bottom deformations take place, predominantly during storms. The bottom slope of the measuring area for the "Norderney'94" experiment is mild (approximately 1:50); hence, the suspended sand flux according to Bailard's model (q_s) has the form:

$$q_s(t) = \frac{\varepsilon_s \cdot f_w \cdot \rho_t \cdot S_0}{g \cdot h \cdot w_s} \cdot \left|u(t)\right|^3 \cdot u(t), \tag{8}$$

where f_w is the wave friction coefficient; $S_0 = \rho/(\rho_t - \rho)$ with ρ_t for the density of the sediment and ρ for the water; g is the acceleration of gravity; w_s represents the settling velocity of the sediment particles; $u(t)$ is the time varying cross-shore velocity and ε_s represents the coefficient of effectiveness. This formula could be rewritten in terms of sediment concentration by weight as:

$$q_s(t) = C_T(t)\, u(t)\,, \tag{9}$$

$$C_T = \frac{\varepsilon_s \cdot f_w \cdot \rho_t \cdot S_0}{g \cdot h \cdot w_s} \cdot \left|u^3(t)\right| \cdot \tag{10}$$

It is convenient to calculate the averaged value of the net suspended sand flux in the cross-shore direction $q_{net} = C_T\, u$ over the duration of a defined time series (the symbol $< >$ denotes the time averaging) as:

$$< C_T(t) \cdot u(t) > = < C_T(t) > < u(t) > + < C_T(t) \cdot u(t) >_L + < C_T(t) \cdot u(t) >_W + < C_T(t) \cdot u(t) >, \tag{11}$$

where the net suspended sediment flux in the cross-shore direction ($< C_T(t)\, u(t) >$) is the sum of the fluxes which are determined by the averaged current ($< C_T(t) >< u(t) >$), by the long waves ($< C_T(t)\, u(t) >_L$), by the short waves ($< C_T(t)\, u(t) >_W$) and by the turbulence ($< C'_T(t)\, u'(t) >$). $C_T(t)$ and $u(t)$ are instantaneous values of the suspended sand concentration and of the cross-shore velocity (KOS'YAN et al., 1997a).

The turbulent cross-shore suspended flux is about one order smaller than the other terms of the equation (11); therefore it may be omitted.

The measured suspended sediment flux can be calculated in a comparable manner:

$$< C_T(t) \cdot u(t) > = < C(t) > < u(t) > + < C(t) \cdot u(t) >_L + < C(t) \cdot u(t) >_W, \tag{12}$$

where $C(t)$ is the time series of measured sediment concentration.

The theoretically determined and the measured values of the fluxes associated with long waves were calculated according to formula (11) and (12) by integration of the values for the co-spectra between the suspended sand concentration and the cross-shore velocity in the frequency range 0.005 Hz $< f <$ 0.05 Hz and those fluxes associated with short waves in the frequency range 0.05 Hz $< f <$ 0.5 Hz.

For the calculation we used the measured cross-shore velocities from the "Norderney'94" experiment with time series of one hour duration. We introduced into the formula (10): ρ_t = 2650 kg/m^3; ρ = 1020 kg/m^3; f_w = 0.01; ε_S = 0.02; w_S = 0.028 m/s.

Die Küste, 64 (2001), 161-200

The Figs. 24 to 27 represent four typical situations for the surf zone, which are characterized by cross-shore currents (undertow), with velocities which increase from Fig. 24 to Fig. 27. The results gained with the theoretically determined data are drawn in black, and those based on the field data are shown in white; positive values characterize the onshore and negative values the offshore direction. Four averaged values are distinguished: transport by "long" waves and by "short" waves; "mean" transport and "net" transport.

Fig. 24 applies for the case, where the undertow velocity is nearly zero and the main contribution to the net suspended sand flux is provided by the infragravity (long) waves. In this case, the r.m.s. values (based on field data) of the suspended sand fluctuations are equal to 1.15 kg/m^{2}s, which is approximately ten times more than the displayed net flux. In contrary, the main contribution to the net suspended sand flux which has been calculated by the model, is provided by the short waves.

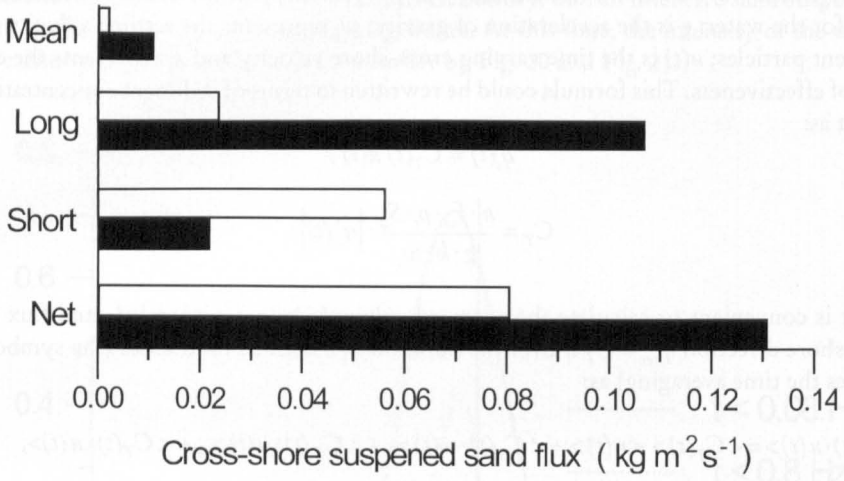

Fig. 24: Suspended sand fluxes in cross-shore direction : measured (white) and predicted by Bailard's model (black). – "Norderney'94" experiment; time series of 60 minutes: H_s = 0.80 m; T_p = 8.7 s; h = 1.14 m; flat bottom; undertow velocity $\langle u \rangle$ = 0.01 m/s

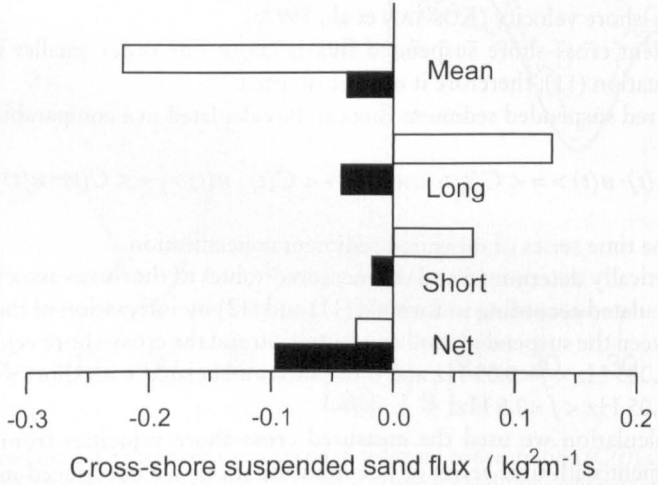

Fig. 25: The same as Fig . 24, but for: H_s = 0.84 m; T_p = 9.7 s; h = 1.16 m; $\langle u \rangle$ = –0.1 m/s.

Die Küste, 64 (2001), 161-200

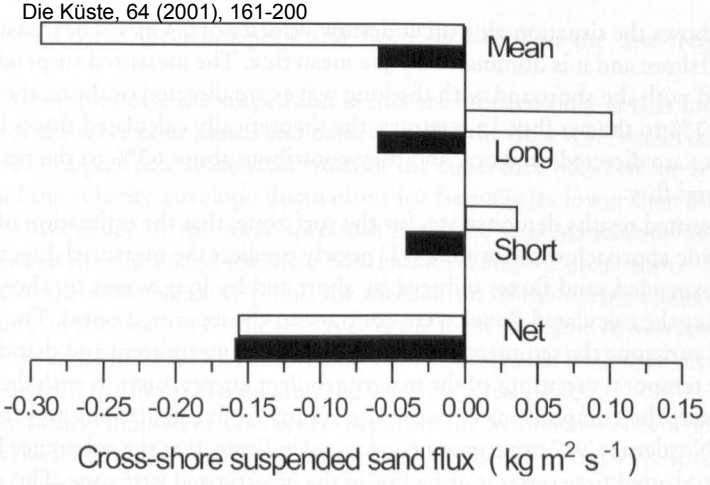

Fig. 26: The same as Fig . 24, but for: H_s = 1.31 m; T_p = 9.8 s; h = 2.05 m; $\langle u \rangle$ = −0.18 m/s

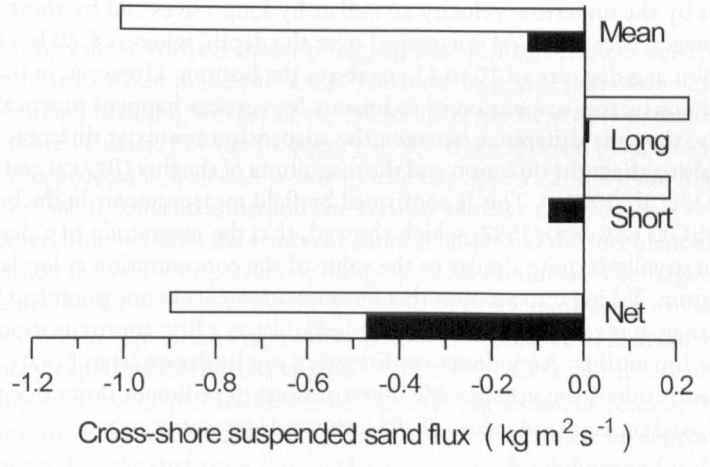

Fig. 27: The same as Fig . 24, but for: H_s = 1.42 m; T_p = 9.8 s; h = 2.30 m; $\langle u \rangle$ = −0.40 m/s

Fig. 25 demonstrates analogous data for a case with an undertow velocity equal to 0.1 m/s. The measured sand fluxes by the short and by the long waves are directed onshore, and they almost completely compensate the offshore-directed transport by the mean flow. The r.m.s. values of the suspended sand flux fluctuations are equal to 1.25 kg/m^{2}s, which is close to the previous case. The model predicts the suspended sand fluxes by short and by long waves which are also directed onshore, but in contrary to the measured fluxes with almost equal values; the resulting net flux calculated with the model is three times larger than the measured one.

Fig. 26 presents the results for an undertow velocity of 0.18 m/s. The measured net suspended sand flux is directed offshore. Values of the fluxes by short and by long waves are predicted by the model almost in the same order and both are directed offshore, in contrary to the measured fluxes (analog to the preceding case). The values of the predicted and of the measured "net fluxes" are nearly the same, but the model – predicted values and directions of the flux-components (fluxes by short waves, by long waves and by the mean current) do not coincide with the measured ones.

Die Küste, 64 (2001), 161-200

Fig. 27 shows the situation with an undertow velocity of 0.4 m/s. The measured net flux is directed offshore and it is dominated by the mean flux. The measured suspended sand fluxes associated with the short and with the long waves are directed onshore; they contribute only about 10 % to the net flux. In contrary, the theoretically calculated fluxes by short and by long waves are directed offshore, and they contribute about 60 % to the net cross-shore suspended sand flux.

The presented results demonstrate, for the surf zone, that the estimation of sand fluxes by the energetic approach with formula (11) poorly predicts the measured directions and values of the suspended sand fluxes induced by short and by long waves (in three of the four discussed cases the calculated fluxes were contrary to the measured ones). The main reason is, that in the surf zone the sediment fluctuations are very intermittent and that they coincide well with the temporal variations of the macroturbulent energy, but not with the cross-shore velocity. Hence, the comparisons between the results from calculations and from the field data of the "Norderney'94" experiment (surf zone) indicate, that the coherence between calculated and measured time series is quite low in the investigated surf zone. This result can be generalized and transferred to surf zones of other locations.

It is necessary to note, that a quantitative comparison between the measured and the calculated fluxes by the undertow velocity as well as by long waves and by short waves is not absolutely correct, because $C_T(t)$ is averaged over the depth, whereas $C(t)$ has been measured in one point at a distance of 10 to 15 cm above the bottom. However, in the wave breaking zone the convective suspension of sediments by vortices happens practically instantly. Consequently, the time difference between the suspension events at different levels is too short to be able to affect the direction and the magnitude of the flux (BEACH and STERNBERG, 1988; KOS'YAN et al., 1997 a). This is confirmed by field measurements in the breaking zone (OSBORN and GREENWOOD, 1992) which showed, that the magnitude of a depth-averaged concentration usually is quite similar to the value of the concentration at levels 10 to 20 cm above the bottom. Taking into account that our measurements in one point had been performed in this range, it is reasonable to use these field data as a first approximation for calculations of the sediment flux. An indirect confirmation can be drawn from FOOTE et al. (1995), who published results from comparable investigations of sediment flows due to short and long waves, based on averaged values of the measured concentrations.

6. Conclusions

The processes which control the temporal variability of the suspended sand concentration near the bottom under the influence of tides and waves, have been examined by using field data. Optical and electromagnetic sensors with a high frequency response performed the measurements.

The lee vortex ejection is the basic mechanism of sand suspension for low energetic conditions in nearshore zones with slightly shoaling waves and a rippled bed. The suspension events coincide well with groups of high waves.

For the 2D ripples case the suspension events occurred twice per period and coincided with the time of the flow reversal.

Statistically significant values of coherence between the suspended sand and the cross-shore velocity fluctuations are recognized for the frequency of the wave spectrum peak and for the frequency of the waves group. At these frequencies, the sediment concentration fluctuations lead the cross-shore velocity and its envelope by approximately $-\pi/2$ at the

Die Küste, 64 (2001), 161-200

frequency of the wave spectrum peak and from $-\pi/2$ to 0 in the low-frequency band < 0.8 Hz.

For the 3D ripples case the suspension events are induced only at that moment, when the backside of the wave crest passes and coincidentally the flow reverses. From a comparison with the 2D ripples case some reductions of the coherence between the sediment concentration and the velocity envelope fluctuations for frequencies lower than 0.1 Hz are observed. At the frequency of the wave spectrum peak, the same conclusion applies for the phase lag between the suspended sediment concentration and the cross-shore velocity.

Seaward of the wave breaking point, the mechanism of the vortex ejection due to the shear instability of the bottom boundary layer is the most probable reason for the entrainment of sand from the bottom. The suspension events coincide in time with the flow decelerating phase or with the flow reversal after the wave crest has passed.

The statistically significant coherence between the sediment concentration and the cross-shore velocity has been confirmed for the peak frequency of the wave spectrum as well as for its first harmonic. The sediment concentration follows the velocity fluctuations with a phase lag of $-\pi/4$ at the frequency of the wave spectrum peak. At the low frequency band ($f < 0.08$ Hz), the sediment concentration correlates poorly with both the velocity and its envelope.

The macroturbulent vortices under plunging and spilling breakers determine the mechanism of sand suspension in the surf zone. The most intensive suspension events are formed under plunging breaking waves. These events correspond in time to the forward front of the cross-shore velocity. For the frequency of the wave spectral peak and for the lower frequencies, this process is well confirmed by the Co-Spectra and by the high coherence between the sediment concentration and the vertical velocity component.

A high correlation between the sediment concentration and the turbulent kinetic energy is observed inside the surf zone, where spilling breakers dominate. The largest suspension events are created by the vortices when the turbulent velocity some times exceeds its r.m.s. -value. This result is in a qualitative agreement with the turbulence data under breaking waves in laboratory experiments (TING and KIRBY, 1995, 1996; COX and KOBAYASHI, 1999).

In existing models, the prediction of the time varying sediment concentration is based on a near-bottom "reference concentration", which is determined in dependency of the Shields parameter. For the surf zone, it is doubtful to use such a definition for the "reference concentration" because the sediment concentration is weakly coherent to the time varying cross-shore velocity.

In the shoaling wave zone, the discussed definition of the "reference concentration" may be used for modeling the time varying sediment transport, because in this zone the sediment concentration fluctuations correlate well with the cross-shore velocity. But it is necessary to take into account the vertical convection of the suspended sand and also the phase lag between concentration and velocity.

From the physical point of view, it is the most effective way to understand the sand suspension process and to predict the sand concentration fluctuations, to determine the relationships between concentration and macro turbulence parameters as well as between the macroturbulent parameters and the dissipation of wave energy by breaking. To obtain such relations, it is necessary to investigate the spatial-temporal variability of the macro turbulence and of the sand suspension under breaking irregular waves.

Die Küste, 64 (2001), 161-200

7. Acknowledgement

This paper appears under the financial support of the NATO Science Program "Partnership for the peace", Linkage Grant No 974562: "Cross-shore sediment transport: physical regularities and modeling". The performance of the field experiments was supported by the Department of Life and Earth Sciences of the Ministry of Industry, Science and Technologies of the Russian Federation, by the German Federal Ministry for Education and Research (BMBF) and by the International Center for Coastal Resources Research (CIIRC), Barcelona, Spain. The "Norderney'94"-experiment was part of the KFKI (Kuratorium für Forschung im Küsteningenieurwesen) – Project on Beach Nourishment ("Vorstrand- und Strandauffüllungen im Bereich von Buhnen – Deckwerkssystemen").

8. References

BAILARD, J. A.: An energetic total load sediment transport model for a plane sloping beach. J. Geophys. Research, 86(C11), 10938–10954, 1981.

BAKKER, W. T.: Sand concentration in an oscillatory Flow. Proc. 14th Int. Conf. on Coastal Engineering, ASCE, 1129–1148, Copenhagen, 1974.

BEACH, R. A. and STERNBERG, R. W.: Suspended sediment transport in the surf zone: Response to cross-shore infragravity motion. Mar.Geol., 80, 671–679, 1988.

CANTWELL, B. J.: Organized motion in the turbulent flow. Ann. Rev. Fluid Mech., 13, 457–515, 1981.

CONLEY, D. C. and INMAN, D. L.: Field observation of the fluid granular boundary layer under near breaking waves. J. of Geophysical Research, 97 (C6), 9631–9643, 1992.

COX, D. T. and KOBAYASHI, N.: Coherent motion in the bottom boundary layer under shoaling and breaking waves. Proc. 26th Int. Conf. on Coastal Engineering, Copenhagen, ASCE, 457–470, 1999.

COX, D. T. and KOBAYASHI, N.: Identification of intense, intermittent coherent motion under shoaling and breaking waves. J. Geophys. Research, 105(C6), 14223–14236, 2000.

DAVIES, A. G.: Modeling the vertical distribution of suspended sediment in combined wave-current flow. In: Dynamics and Exchanges in Estuaries and the Coastal zone, Coastal and Estuarine Studies, vol. 40, Ed. D. Prandle, AGU, 441–466, Washington, 1992.

DAVIES, A. G. and LI, Z.: Modeling sediment transport beneath regular symmetrical and asymmetrical waves above a plane bed. Continental Shelf Research, 17 (5), 555–582, 1997.

DEIGAARD, R.; FREDSOE, J. and HEDEGAARD, B.: Suspended sediment in the surf zone. J.Waterway, Port, Coastal and Ocean Engineering, ASCE, 112, 115–128, 1986.

FOOTE, Y. L. M.; HUNTLEY, D. H. and O'HARE, T.: Sand transport on macrotidal beaches. Proceedings of Euromech 310 colloquium, 360–374, Le Havre, 1995.

FOSTER, D. L.; HOLMAN, R. A. and BEACH, R. A.: Sediment suspension events and shear instabilities in the bottom boundary layer. Proceedings of the International Conference on Coastal Research in Terms of Large Scale Experiments, "Coastal Dynamics' 94", ASCE, 712–716, Barcelona, 1994.

FREDSOE, J.; ANDERSEN, O. H. and SILBERG, S.: Distribution of suspended sediment in large waves. J. Waterway, Port, Coastal and Ocean Engineering, ASCE, 111, 1041–1059, 1985.

GEORGE, K.; FLICK, R. E. and GUZA, R. T.: Observation of turbulence in surf zone. J. of Geoph. Res., Vol. 99 (C1), 801–810, 1994.

HAGATUN, K. and EIDSVIK, K. J.: Oscillating turbulent boundary layer with suspended sediment. J. Geophys. Research, 91(C11), 13045–13055, 1988.

HANSEN, E. A.; FREDSOE, J. and DEIGAARD, R.: Distribution of suspended sediment over wave-generated ripples. J. Waterway, Port, Coastal and Ocean Engineering, ASCE, 120, 37–55, 1994.

HINO, M.; KASHIWAYANAGI, M.; NAKAYAMA, A. and HARA, T.: Experiments on the turbulence statistics and the structure of reciprocating oscillatory flow. J. Fluid Mech. Vol. 131, 363–400, 1983.

KANEKO, A.: Oscillation sand ripples in viscous fluids. Proc. Jap. Soc. Civ. Eng., Vol. 307, 113–124, 1981.

KOS'YAN, R. D.: Study of sand microforms in the nearshore zone. Marine Geology, Vol. 83. 63–78, 1988.

KOS'YAN, R. D. and PYKHOV, N. V.: Hydrogenous sediment shift in the coastal zone. Moscow, "Nauka" Publ., 1991., 280 p. (in Russian).

KOS'YAN, R. D. and KOCHERGIN, A. D.: About conditions for the wave ripple existence. Proc. of the 23rd Int. Conf. on Coastal Engineering, 2176–2190, Venice, 1992.

KOS'YAN, R. D.; Kuznetsov, S. YU. and PYKHOV; N. V.: Low-frequency fluctuation of suspended sand and wave groups in the surf zone. Proc. of the Second Int. Symp. "Ocean Wave Measurements and Analysis", ed. by O. T. Magoon and J. M. Hemsley. Publ. by ASCE, 352–363, New York, 1994.

KOS'YAN, R. D.; KUZNETSOV, S. YU.; PODYMOV, I. S.; PYKHOV, N. V.; PUSHKAREV, O. V.; GRISHIN, N. N. and HARIZOMENOV D. A.: Optical device for measuring of suspended sediment concentration during a storm in the coastal zone. Oceanology, Vol. 35, N 3, 463–469 (in Russian), 1995.

KOS'YAN, R.; KUNZ, H. and PODYMOV, I.: Employment of electronic sand level gauges for measurement of beach slope deformation on Norderney island. Proceedings of the International Conference on Coastal Research in Terms of Large Scale Experiments, "Coastal Dynamics' 95", ASCE, 651–663, New York, 1996.

KOS'YAN, R. D.; KUNZ, H.; KUZNETSOV, S. YU. and PYKHOV, N. V.: Net suspended sediment transport in the surf zone. Proc. 2nd Indian National Conference on Harbor and Ocean Engineering, "Inchoe' 97", 1073–1085, 1997(a).

KOS'YAN, R. D.; KUNZ, H.; KUZNETSOV, S. YU.; PYKHOV, N. V. and KRYLENKO, M. V.: Sand Suspension and Intermittence of Turbulence in the Surf Zone. Proc. of the 25th International Conference on Coastal Engineering, "COASTAL ENGINEERING' 96". ASCE, 4111–4119, New York, 1997(b).

KOS'YAN, R.; KUNZ, H.; PODYMOV, I. and PYKHOV, N. V.: Sand bottom erosion in the surf zone of Norderney island. Proc. of the Third International Conference on the Mediterranean Coastal Environment, "MEDCOAST' 97". 1263–1273, Malta, 1997(c).

KOS'YAN, R. D. and PODYMOV, I. S.: Sand level gauge. Russian Patent of Invention # 2072539, 1997(d).

KOS'YAN, R. D.; KUZNETSOV, S. YU.; PODYMOV, I. S.; PUSHKAREV, O. V. and PYKHOV, N. V.: Marine turbidimeter. Russian Patent of Invention # 2112232, 1999(a).

KOS'YAN, R. D.; PODYMOV, I. S. and KUZNETSOV, S. YU.: Turbidimetric measuring of the suspended sediment concentration in the coastal zone. Proc. of the 26th International Conference on Coastal Engineering, "COASTAL ENGINEERING' 98", ASCE, Vol. 2, 2303–2316, Virginia, 1999(b).

KOS'YAN, R. D.; PYKHOV, N. V. and EDGE, B. L.: Coastal processes in tideless seas. ASCE Press, Virginia, 2000, 316 p.

KUNZ, H.: The Norderney field investigations for the improvement of beach- and foreshore nourishments. Proc. of the Second German-Chinese joint seminar on recent developments in coastal engineering – Sustainable development in the coastal zone. 495 and appendix A1–A16, Tainan, Taiwan, 1999.

KUNZ, H. and KOS'YAN, R.: German-Russian nearshore dynamics experiment on Norderney island. Proc. of the Third International Conference on the Mediterranean Coastal Environment, "MEDCOAST' 97". 1301–1315, Malta, 1997.

KUZNETSOV, S. YU. and PYKHOV, N. V.: Spectral Test of the Energetic Approach for Suspended sand Transport in the "Surf Zone", Proceedings of the International Conference on Coastal Research in Terms of Large Scale Experiments, "Coastal Dynamics' 97", 227–234, Plymouth,1998.

MARPL, S. L.: Digital spectral analysis. Prentice-Hall, Inc., 1987. 584 p.

MURRAY, P. B.; DAVIES, A. G. and SOULSBY, R. L.: Sediment pick-up in wave and current flows. Proc. of EUROMECH 262 Colloquium on sand transport in rivers, estuaries and the sea (Ed. by R. L. Soulsby and R. Bettes), A. A. Balkema, 37–43, Rotterdam, 1991.

NADAOKA, K. and KONDOH, T.: Turbulent flow field structure of breaking waves in the surf zone. J. Fluid Mech., 204, 359–387, 1989.

NIELSEN, P.: Coastal bottom boundary layers and sediment transport. Word Scientific Publ., 324 p. Hong-Kong, New Jersey, London, Singapore, 1991.

NIHEI, Y.; NADAOKA, K.; YAGI, H. and NOMOTO, K.: Turbulent structure of asymmetric flow. 27th International Conference on Coastal Engineering, Sydney, Australia, Book of Abstracts, V. 2, Poster Nº 35, 2000.

OSBORN, P. D. and GREENWOOD, B.: Frequently dependent cross-shore suspended sediment transport: 1. A non-barred shoreface. Mar.Geol., 106, 1–24, 1992.

PYKHOV, N. V.; KOS'YAN, R. D. and KUZNETSOV, S. YU.: Time scales of sand suspending by irregular waves. Proc. of the Second International Conference on the Mediterranean Coastal Environment, "MEDCOAST' 95". 1073–1091, Tarragona, Spain, 1995.

PYKHOV, N. V.; KUZNETSOV, S. YU. and KUNZ, H.: Mechanisms of sand suspending under nonbreaking and under breaking irregular waves. Proceedings of the International Conference on Coastal Research in Terms of Large Scale Experiments, "Coastal Dynamics' 97". ASCE, 19–27, Plymouth, 1998.

RIBBERINK, J. S. and AL-SALEM, A.: Sheet flow and suspension of sand in oscillatory boundary layers. Coastal engineering, 25, 205–225, 1995.

RODRIGUES, A.; SANCHEZ-ARCILLA, A.; GOMEZ, J. and BAHIA, E.: Study of surf-zone macroturbulence and mixing using Delta'93 field data. Proceedings of the International Conference on Coastal Research in Terms of Large Scale Experiments, "Coastal Dynamics' 95" 305–316, Gdansk, Poland, 1995.

SANCHEZ-ARCILLA, A.; RODRIGUES, A.; SANTAS, J. C.; GRASIA, V.; KOS'YAN, R.; KUZNETSOV, S. and MOSCO, C.: Delta'96: surf zone and nearshore measurements at the Ebro delta. Proceedings of the International Conference on Coastal Research in Terms of Large Scale Experiments, "Coastal Dynamics' 97". ASCE, 556–565, Plymouth, 1998.

SLEATH, J. F. A.: Sea bed mechanics. Willey. N 4. 355 p., New York, 1984.

SOULSBY, R. L.: The 'Bailard' sediment transport formula: comparisons with data and models. Abstracts-in-depth of Final Overall Meeting the G8-Coastal Morphodynamic Project (MAST-II). 2-46-50, 1995.

SYUNSUKE, I. and ASAEDA, T.: Sediment suspension with rippled bed. J. Hydr.Eng., 109, 409–423, 1983.

TING, F. C. K and KIRBY, J. T.: Observation of undertow and turbulence in a laboratory surf zone. Coastal Eng., 24, 51–80, 1994.

TING, F. C. K and KIRBY, J. T.: Dynamics of surf zone turbulence in a strong plunging breaker. Coastal Eng., 24, 177–204, 1995.

TING, F. C. K. and KIRBY, J. T.: Dynamics of surf zone turbulence in spilling breaker. Coastal Eng., 27, 131–160, 1996.

TUNSTALL, E. B. and INMAN, D. J.: Vortex Generation by Oscillatory flow over rippled surfaces. J. of Geoph. Res., Vol. 80, N 24, 3475–3484, 1975.

ZHANG, P.; SUNAMURA, T.; TANAKA, S. and YAMAMOTO, K.: Laboratory experiment of longshore bars produced by breaker-induced vortex action. Proceedings of the International Conference on Coastal Research in Terms of Large Scale Experiments, "Coastal Dynamics 94", ASCE, 29–43, Barcelona, Spain, 1994.